

Supplementary materials

Table S1: Percentages of each autosome classified as a neutral using *Trendsetter* with a linear ($d = 2$) trend penalty across global human populations. *Trendsetter* was trained with three classes: neutral, hard sweep, and soft sweep.

Chromosome	LWK	YRI	GIH	TSI	CEU	CHB	JPT
1	89.54	91.72	91.58	91.84	92.19	90.03	87.40
2	90.45	92.01	91.90	93.49	91.80	89.56	88.41
3	92.16	91.56	92.40	93.55	92.83	89.44	88.40
4	88.50	89.51	91.16	90.85	90.84	90.67	88.32
5	92.42	91.71	93.32	95.12	94.61	92.92	89.94
6	88.39	87.16	91.70	91.82	92.51	91.63	89.25
7	89.99	90.47	91.72	92.62	92.42	90.65	89.02
8	90.71	91.94	91.10	90.89	91.94	90.67	89.04
9	90.33	91.10	93.25	91.36	91.00	91.59	90.66
10	88.48	89.88	92.21	93.31	93.13	91.29	89.55
11	90.12	91.04	90.41	92.03	92.63	91.70	90.61
12	90.22	91.48	92.07	91.56	91.98	91.31	88.90
13	91.01	91.92	94.01	95.22	94.96	92.14	89.44
14	92.14	92.60	94.20	92.46	92.16	93.32	90.52
15	92.01	92.38	91.29	89.70	89.87	90.24	86.98
16	89.86	90.00	90.95	90.13	91.95	87.78	87.06
17	91.04	90.63	89.80	90.24	91.30	89.11	86.73
18	92.43	92.10	91.47	92.65	91.72	91.48	89.67
19	87.68	87.27	90.40	89.78	90.19	90.10	87.07
20	91.88	91.97	90.16	92.38	91.70	88.15	86.83
21	88.61	89.04	90.53	90.26	91.31	92.00	89.43
22	93.81	92.89	92.71	95.37	94.76	88.49	85.22

Table S2: Percentages of each autosome classified as a hard sweep using *Trendsetter* with a linear ($d = 2$) trend penalty across global human populations. *Trendsetter* was trained with three classes: neutral, hard sweep, and soft sweep.

Chromosome	LWK	YRI	GIH	TSI	CEU	CHB	JPT
1	0.24	0.19	0.56	0.39	0.73	0.37	1.26
2	0.32	0.15	0.48	0.03	0.59	0.47	0.98
3	0.00	0.05	0.65	0.09	0.35	0.30	0.99
4	0.25	0.17	0.72	0.41	1.06	0.42	1.04
5	0.13	0.07	0.39	0.06	0.34	0.18	0.68
6	0.05	0.01	0.87	0.31	1.30	0.52	0.89
7	0.25	0.15	0.48	0.06	0.49	0.42	0.96
8	0.17	0.06	0.45	0.23	0.45	0.14	0.71
9	0.22	0.15	0.35	0.04	0.68	0.04	0.55
10	0.19	0.11	0.50	0.42	0.44	0.40	1.19
11	0.08	0.06	0.98	0.29	0.70	0.33	0.85
12	0.13	0.22	0.54	0.04	0.52	0.18	1.31
13	0.23	0.10	0.23	0.02	0.28	0.26	0.87
14	0.03	0.00	0.27	0.14	0.87	0.13	0.85
15	0.45	0.31	0.38	0.11	0.66	0.74	1.43
16	0.30	0.20	0.66	0.24	0.86	1.08	1.23
17	0.32	0.13	1.14	0.60	0.83	0.39	1.05
18	0.14	0.03	0.87	0.17	0.89	0.05	0.85
19	0.54	0.61	0.56	0.13	0.83	0.15	0.95
20	0.26	0.30	0.68	0.01	0.40	0.52	0.80
21	0.05	0.03	0.73	0.01	0.46	0.29	0.99
22	0.12	0.06	0.74	0.01	0.29	0.14	1.83

Table S3: Percentages of each autosome classified as a soft sweep using *Trendsetter* with a linear ($d = 2$) trend penalty across global human populations. *Trendsetter* was trained with three classes: neutral, hard sweep, and soft sweep.

Chromosome	LWK	YRI	GIH	TSI	CEU	CHB	JPT
1	10.22	8.09	7.86	7.78	7.08	9.60	11.34
2	9.23	7.84	7.62	6.47	7.61	9.97	10.61
3	7.84	8.39	6.95	6.35	6.82	10.26	10.61
4	11.25	10.33	8.12	8.74	8.10	8.91	10.64
5	7.45	8.21	6.28	4.82	5.05	6.90	9.37
6	11.56	12.83	7.43	7.87	6.19	7.85	9.85
7	9.76	9.38	7.80	7.32	7.09	8.93	10.01
8	9.12	8.00	8.46	8.88	7.61	9.19	10.25
9	9.45	8.75	6.40	8.61	8.32	8.37	8.79
10	11.33	10.01	7.29	6.27	6.43	8.31	9.25
11	9.80	8.90	8.61	7.68	6.67	7.97	8.54
12	9.65	8.30	7.39	8.41	7.50	8.51	9.79
13	8.76	7.98	5.76	4.76	4.76	7.60	9.69
14	7.83	7.40	5.53	7.39	6.97	6.55	8.64
15	7.54	7.31	8.33	10.19	9.48	9.02	11.59
16	9.84	9.81	8.40	9.63	7.19	11.15	11.71
17	8.64	9.24	9.07	9.16	7.87	10.50	12.21
18	7.43	7.87	7.66	7.18	7.39	8.47	9.48
19	11.78	12.12	9.05	10.09	8.98	9.75	11.97
20	7.86	7.73	9.16	7.60	7.90	11.33	12.37
21	11.34	10.93	8.74	9.73	8.23	7.71	9.58
22	6.07	7.05	6.55	4.61	4.95	11.38	12.95

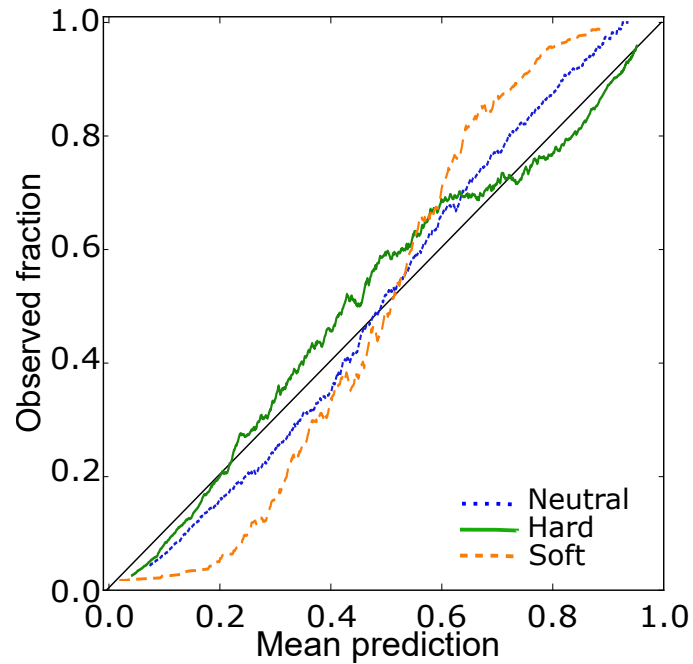


Figure S2: Reliability curves for each of three classes (neutral, hard sweep, and soft sweep) for *Trendsetter* with a linear ($d = 2$) trend penalty trained on data simulated under a constant-size demographic history. For each class we calculate the proportion of observed instances with probability for that class falling within bins of width 0.05 in sliding windows with increments of 0.001 from 0.0 to 1.0, with the first window centered at 0.025 and the last at 0.975.

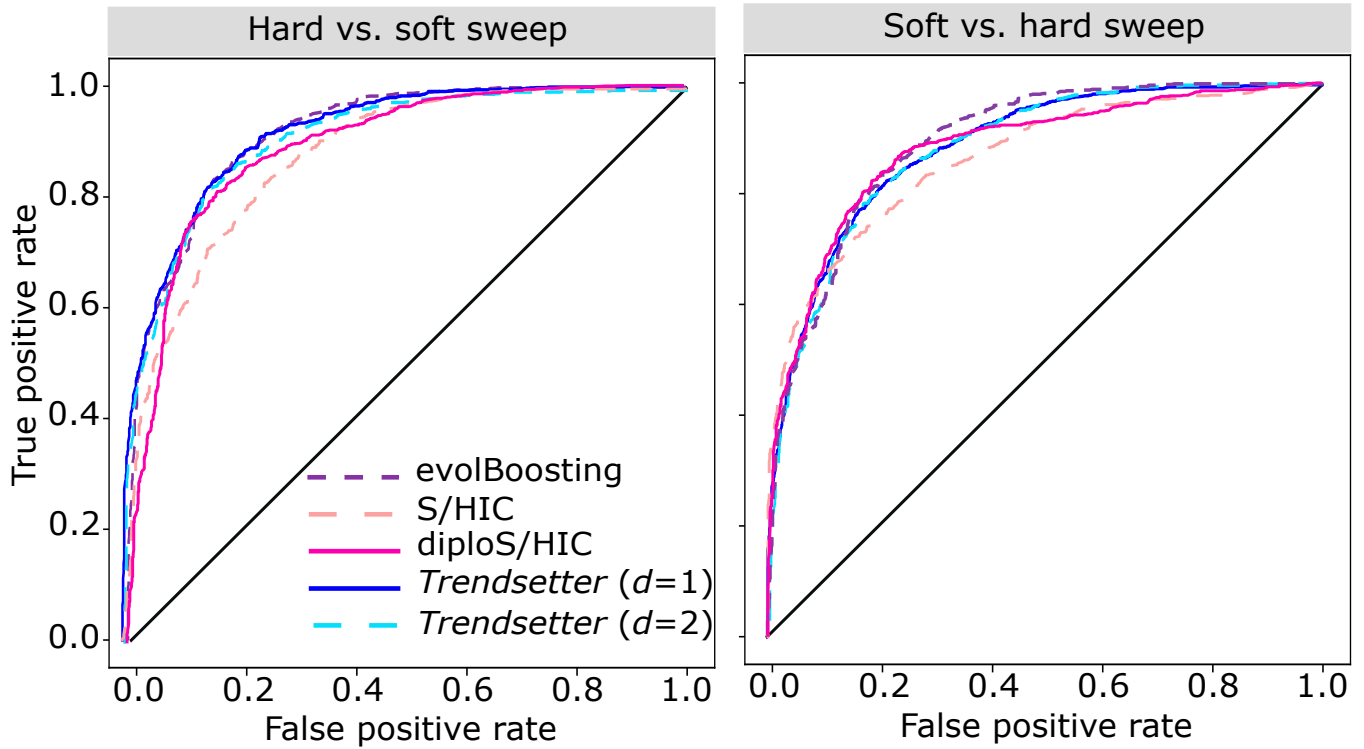


Figure S3: Receiver operating characteristic curves comparing the powers of various methods to distinguish soft sweeps from hard sweeps. (Left) Comparison of the probability of a hard sweep under hard sweep simulations (true positive rate) with the same probability under soft sweep simulations (false positive rate). (Right) Comparison of the probability of a soft sweep under soft sweep simulations (true positive rate) with the same probability under hard sweep simulations (false positive rate). All simulations were performed under a constant-size demographic history with selection coefficients for sweep scenarios drawn uniformly at random on a log scale of $[0.005, 0.5]$. All methods were trained with three classes: neutral, hard sweep, and soft sweep. Note that because we are training *Trendsetter* with three classes, the curves in these two panels do not provide the same information. However, if we instead trained *Trendsetter* using two classes, then one of these curves would have been sufficient.

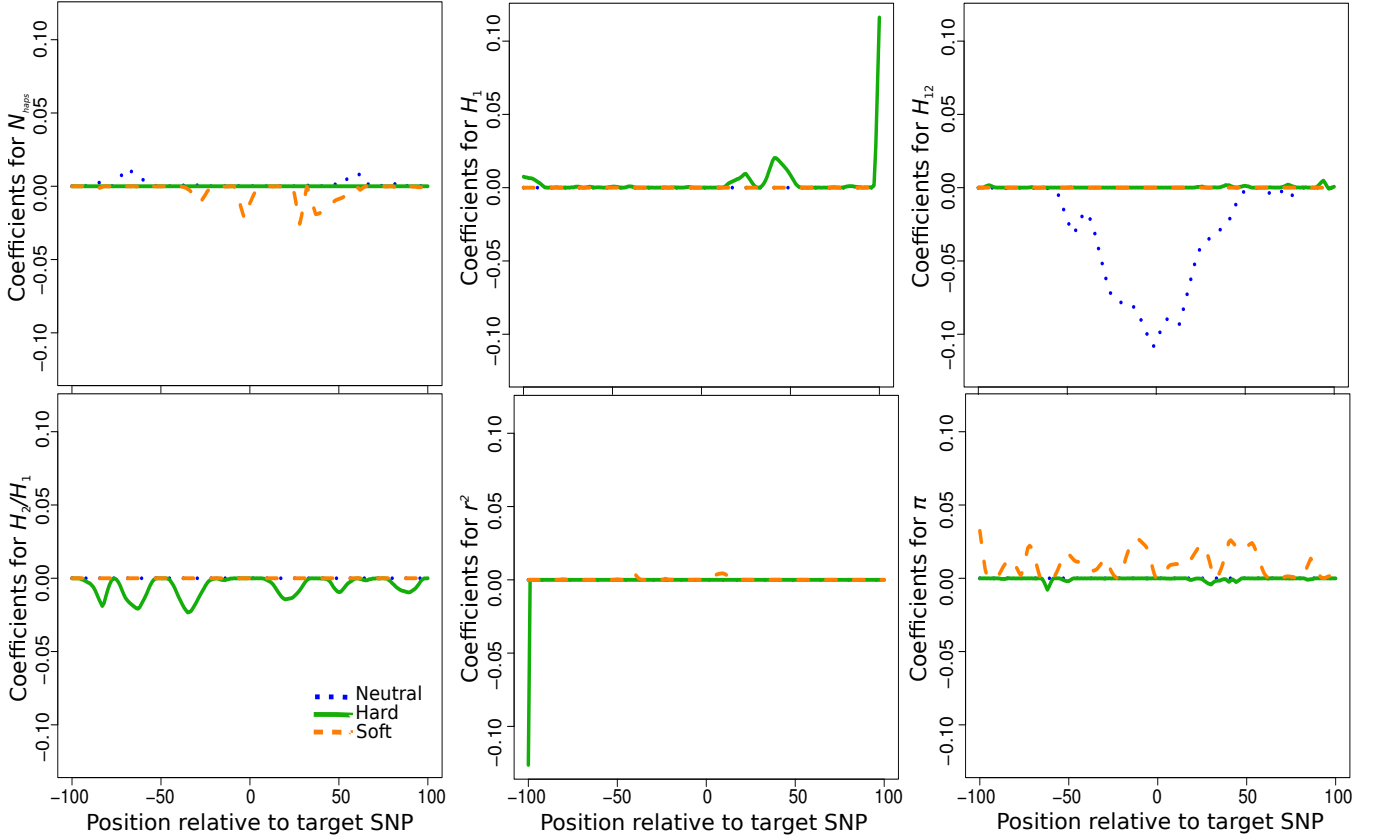


Figure S4: Spatial distributions of regression coefficients (β_s) in neutral, hard sweep, and soft sweep scenarios for summary statistics N_{haps} , H_1 , H_{12} , H_2/H_1 , r^2 , and $\hat{\pi}$, for *Trendsetter* applied with a linear ($d = 2$) trend penalty. *Trendsetter* was trained on simulations with selection strength $s \in [0.005, 0.5]$ sampled uniformly at random on a log scale. Note that the distributions of regression coefficients for all summary statistics are plotted on the same scale, thereby making the distributions of some summaries difficult to decipher as their magnitudes are relatively small.

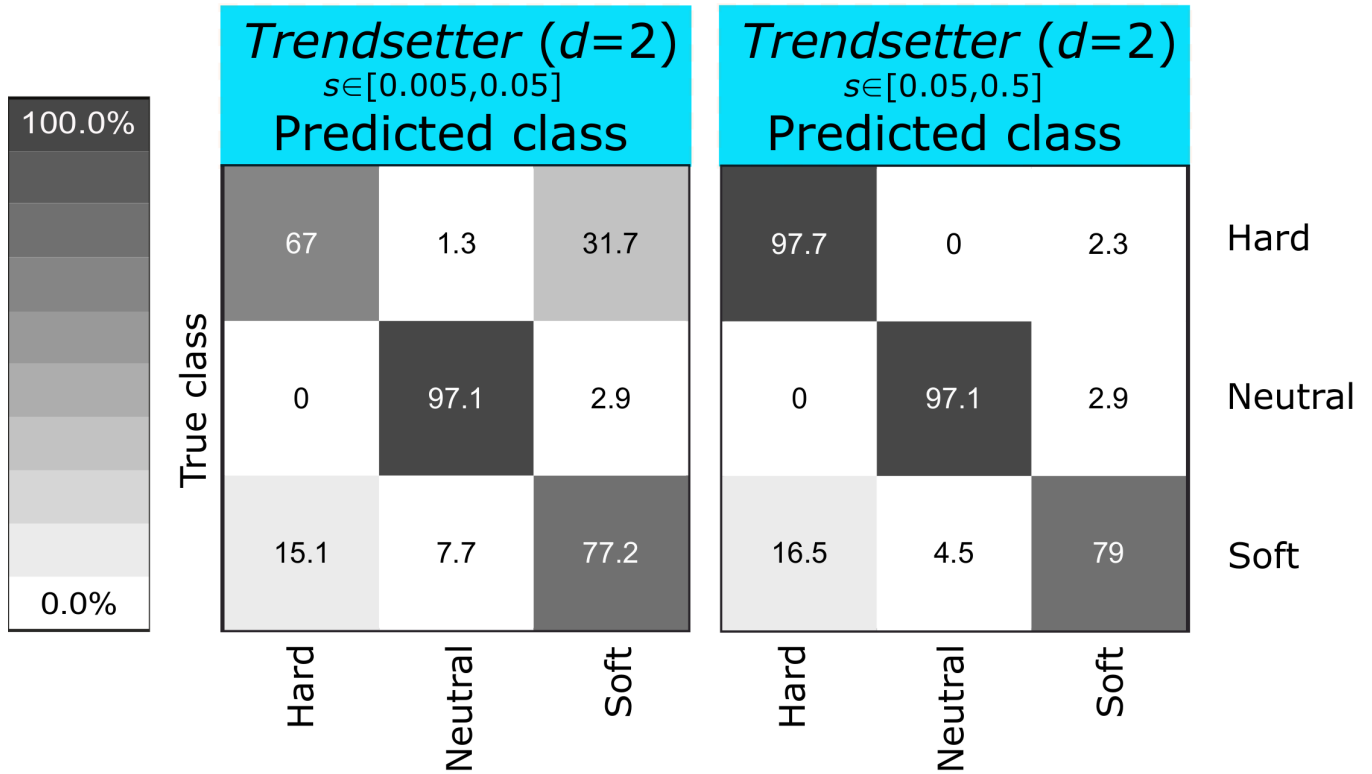


Figure S5: Confusion matrices comparing classification rates of *Trendsetter* with a linear ($d = 2$) trend penalty applied to a scenario in which selection coefficients for sweeps were drawn uniformly at random on either $[0.005, 0.05]$ or $[0.05, 0.5]$. Simulations were performed under a constant-size demographic history. *Trendsetter* was trained with three classes: neutral, hard sweep, and soft sweep, with selection coefficients for sweep scenarios drawn uniformly at random on a log scale of $[0.005, 0.5]$.

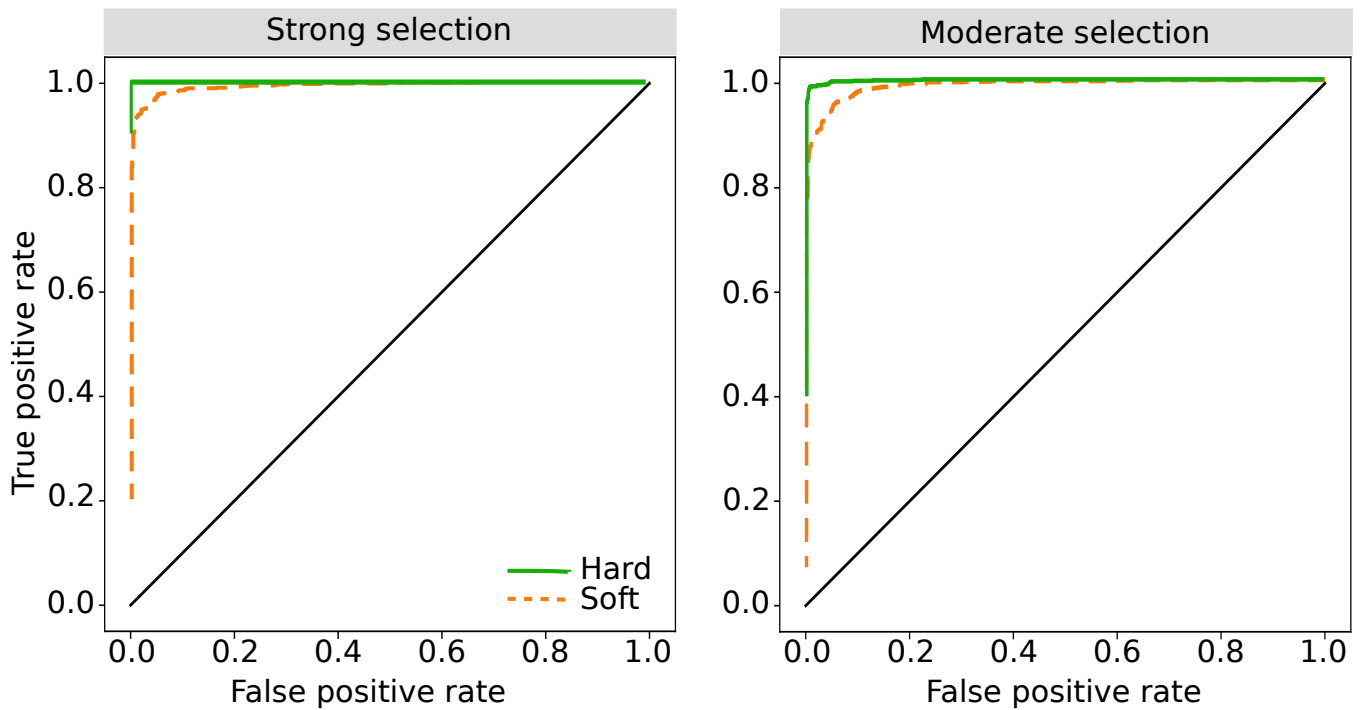


Figure S6: Receiver operating characteristic curves showing the power of *Trendsetter* with a linear ($d = 2$) trend penalty to detect hard and soft sweeps for strong ($s \in [0.05, 0.50]$) and moderate ($s \in [0.005, 0.05]$) selection, under a constant-size demographic history. For hard (soft) sweep curves, we compare the probability of a hard (soft) sweep under hard (soft) sweep simulations with the same probability under neutral simulations.

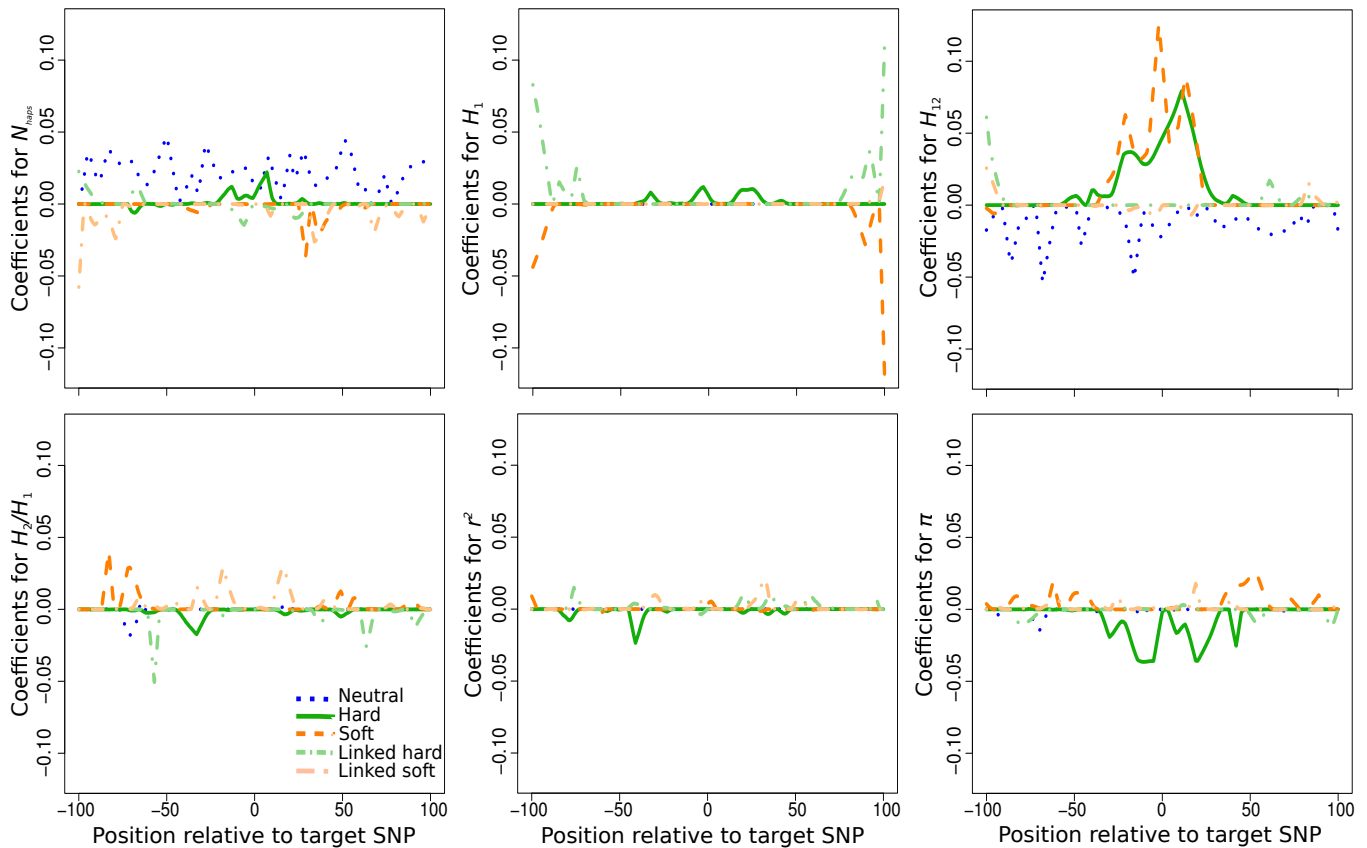


Figure S8: Spatial distributions of regression coefficients (β s) in neutral, hard sweep, soft sweep, linked to hard sweep, and linked to soft sweep scenarios for summary statistics N_{haps} , H_1 , H_{12} , H_2/H_1 , r^2 , and $\hat{\pi}$, for *Trendsetter* applied with a linear ($d = 2$) trend penalty. *Trendsetter* was trained on simulations with selection strength $s \in [0.005, 0.5]$ sampled uniformly at random on a log scale. Note that the distributions of regression coefficients for all summary statistics are plotted on the same scale, thereby making the distributions of some summaries difficult to decipher as their magnitudes are relatively small.

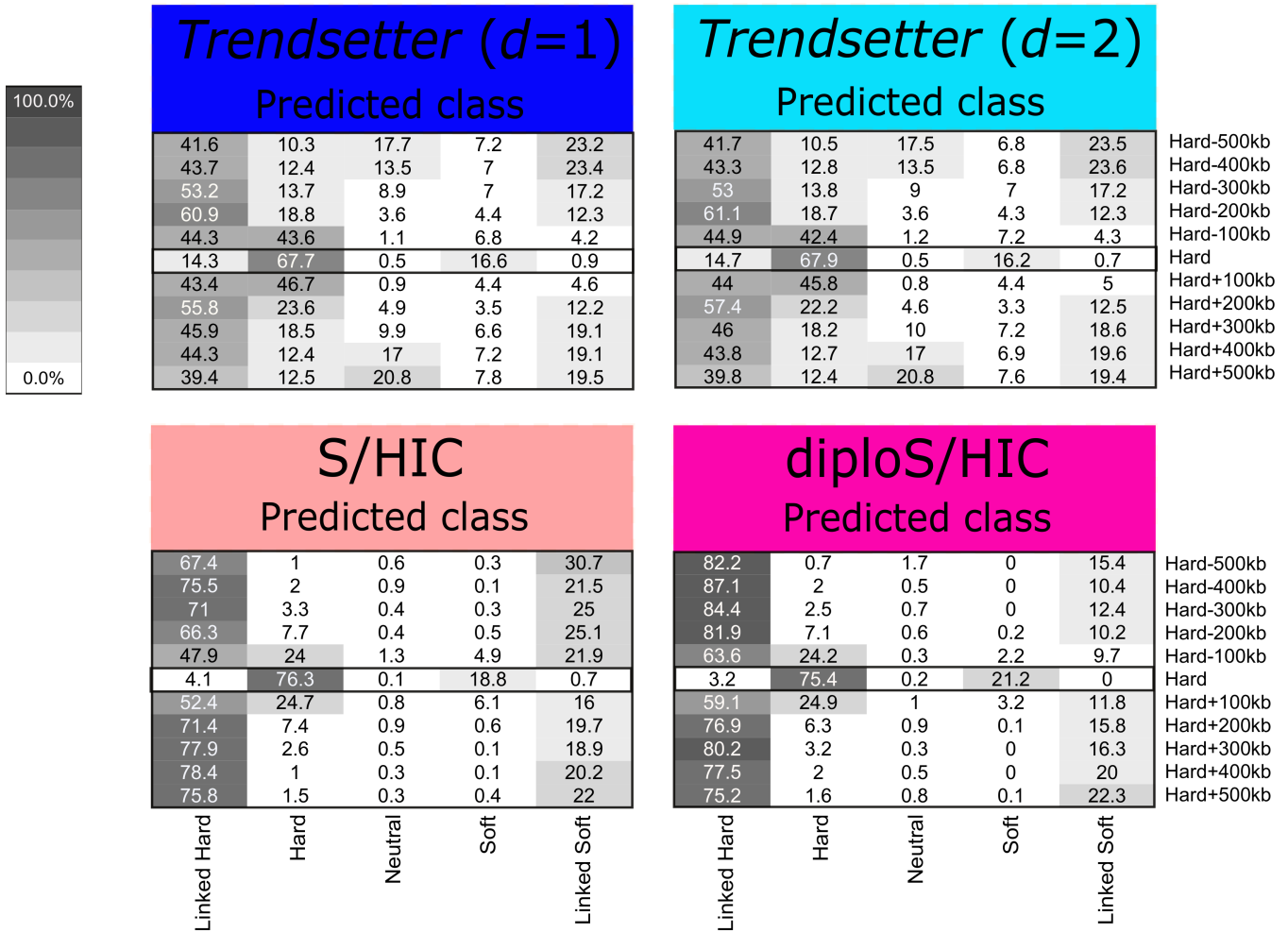


Figure S9: Confusion matrices comparing classification rates of *Trendsetter* with constant ($d = 1$) and linear ($d = 2$) trend penalties, S/HIC, and diploS/HIC applied to regions that are linked to a hard sweep, illustrating their performances under “soft shoulders”. Simulations were performed under a constant-size demographic history and selection coefficients for sweep scenarios drawn uniformly at random on a log scale of $[0.005, 0.5]$. All methods were trained with five classes: neutral, hard sweep, soft sweep, linked to hard sweep, and linked to soft sweep.

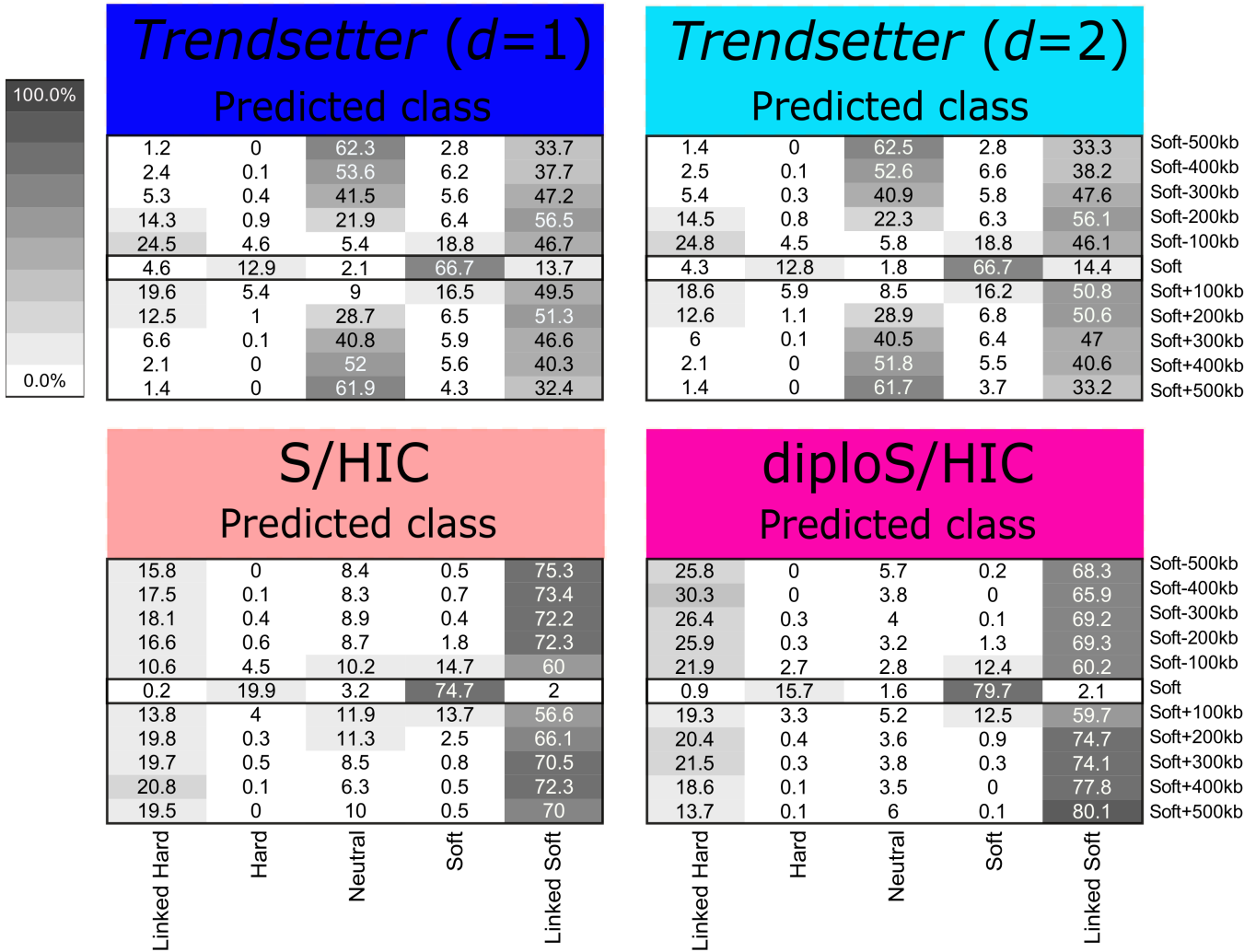


Figure S10: Confusion matrices comparing classification rates of *Trendsetter* with constant ($d = 1$) and linear ($d = 2$) trend penalties, S/HIC, and diploS/HIC applied to regions that are linked to a soft sweep, illustrating their performances under “soft shoulders”. Simulations were performed under a constant-size demographic history and selection coefficients for sweep scenarios drawn uniformly at random on a log scale of $[0.005, 0.5]$. All methods were trained with five classes: neutral, hard sweep, soft sweep, linked to hard sweep, and linked to soft sweep.

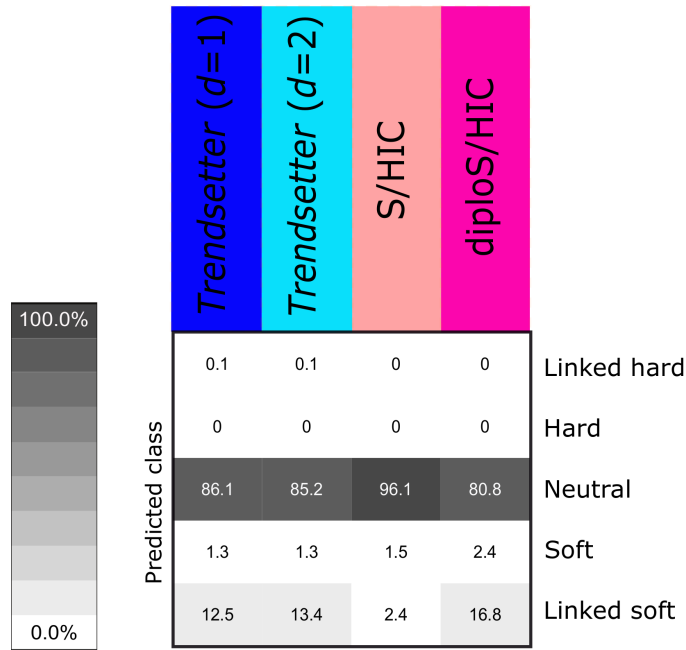
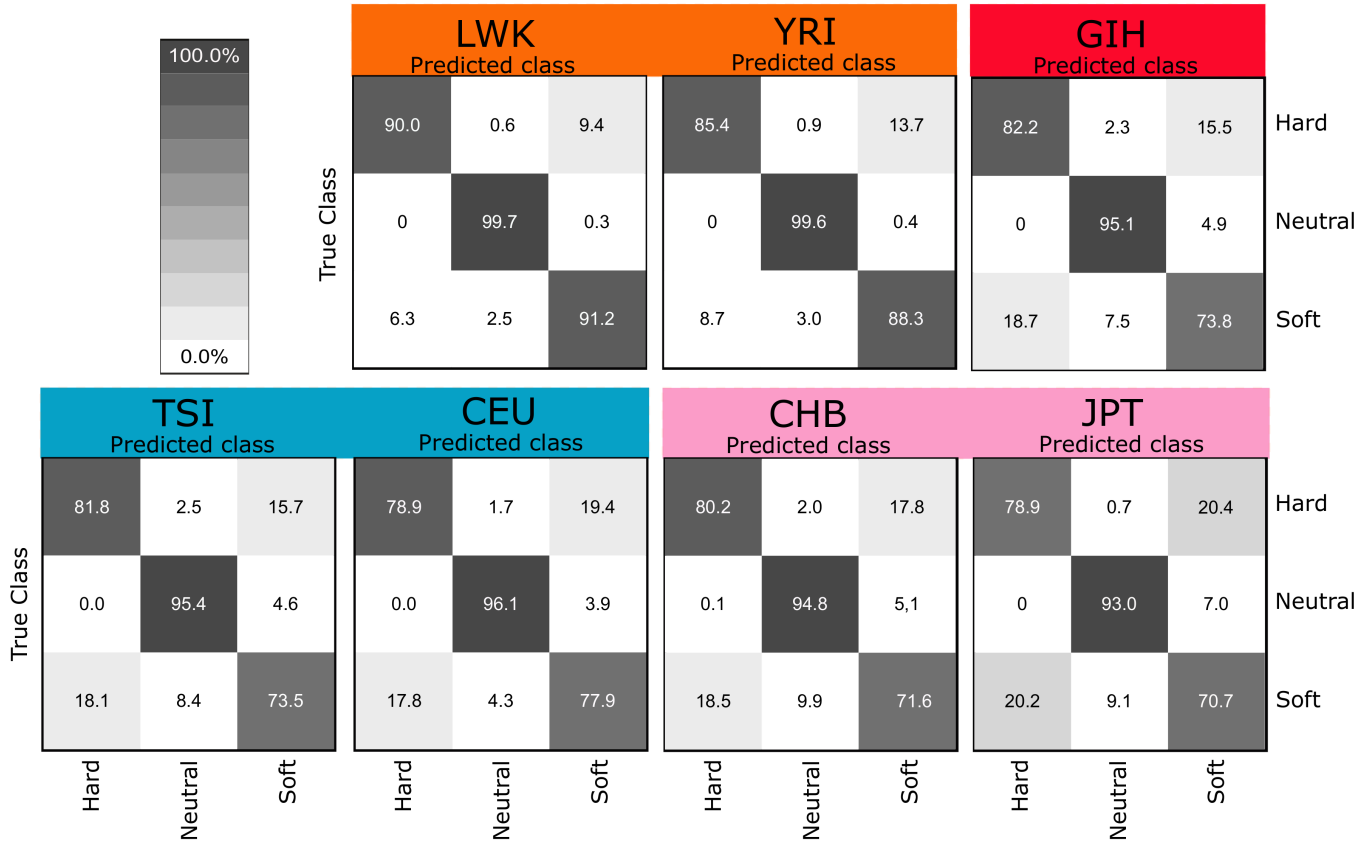


Figure S11: Classification rates of *Trendsetter* with constant ($d = 1$) and linear ($d = 2$) trend penalties, S/HIC, and diploS/HIC applied to neutral regions when trained with five classes: neutral, hard sweep, soft sweep, linked to hard sweep, and linked to soft sweep. Simulations were performed under a constant-size demographic history and selection coefficients for sweep scenarios drawn uniformly at random on a log scale of $[0.005, 0.5]$.



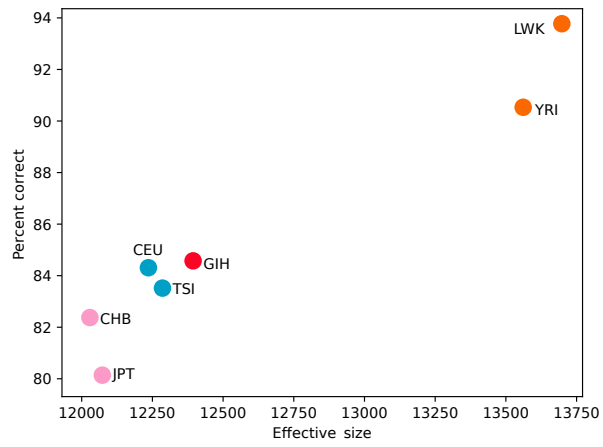


Figure S13: Percentage of correct classifications of *Trendsetter* with a linear ($d = 2$) trend penalty as a function of effective population size of the Terhorst et al. (2017) demographic history analyzed.

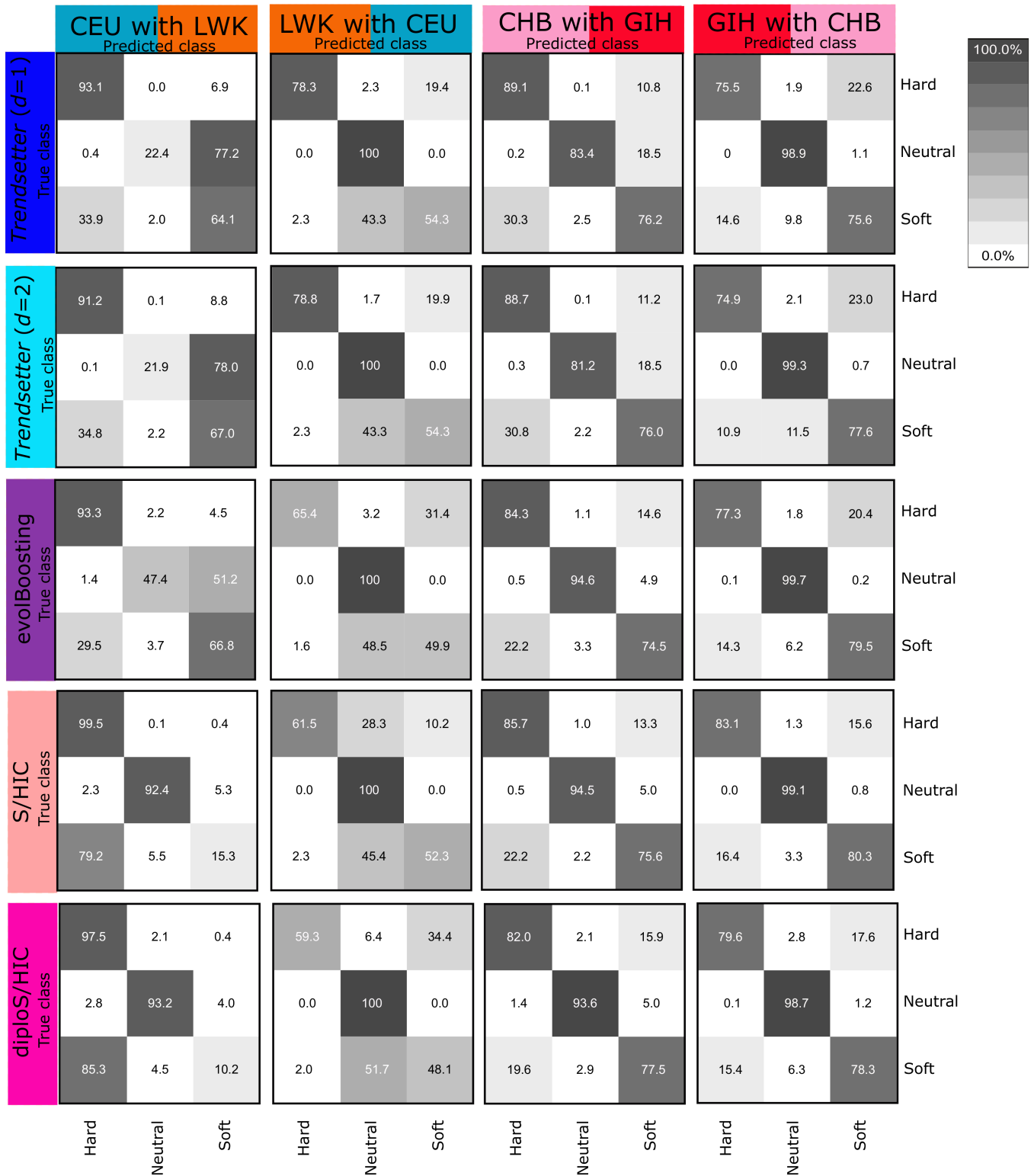


Figure S14: Confusion matrices comparing classification rates of *Trendsetter* with constant ($d = 1$) and linear ($d = 2$) trend penalties, evolBoosting, S/HIC, and diploS/HIC under demographic mis-specification (*i.e.*, testing on a population history that is different from the one that was used to train the classifier). The column label indicates the test population followed by the training population. All methods were trained with three classes: neutral, hard sweep, and soft sweep, with selection coefficients for sweep scenarios drawn uniformly at random on a log scale of $[0.005, 0.5]$.

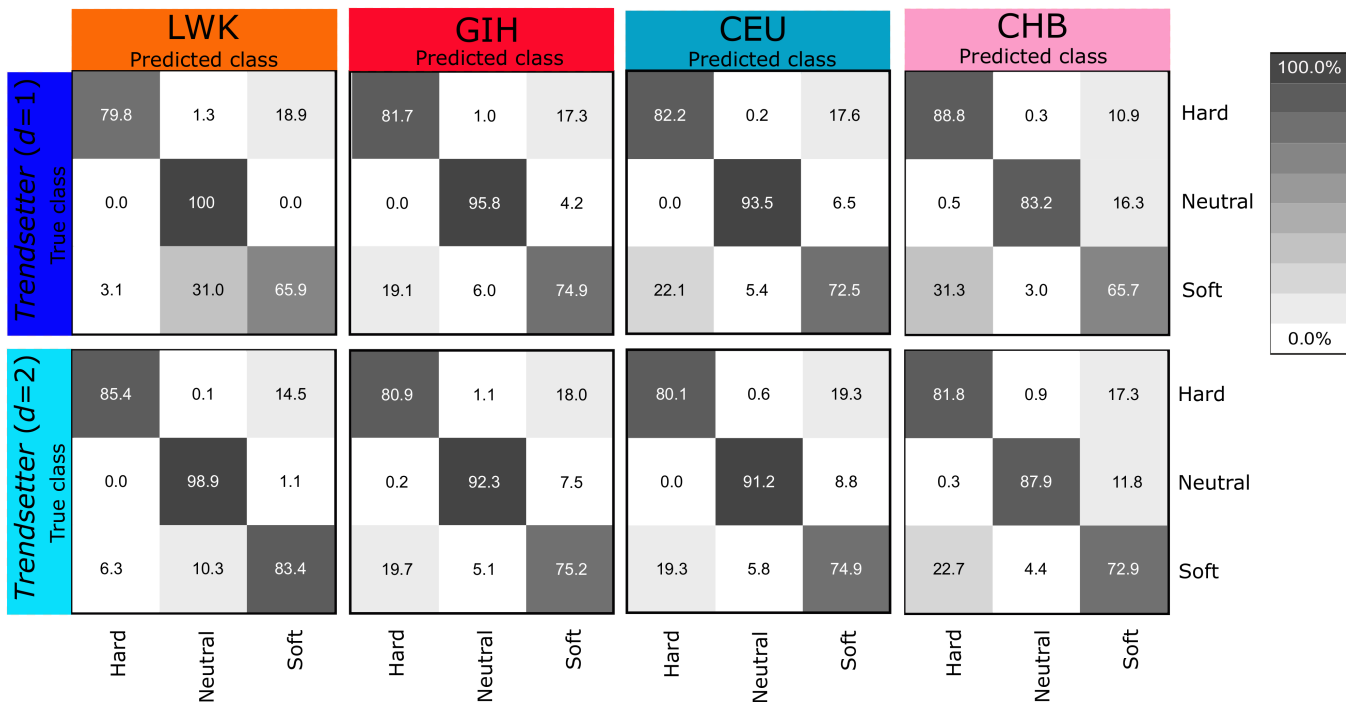


Figure S15: Confusion matrices comparing classification rates of *Trendsetter* with constant ($d = 1$) and linear ($d = 2$) trend penalties under demographic mis-specification when trained on a diverse set of demographic histories. The training dataset consisted of simulations performed under demographic specifications for LWK (African), GIH (South Asian), CEU (European), and CHB (East Asian). Each population comprised a quarter of the 10^3 training simulations for each class. The column label indicates the test population. All methods were trained with three classes: neutral, hard sweep, and soft sweep, with selection coefficients for sweep scenarios drawn uniformly at random on a log scale of $[0.005, 0.5]$.

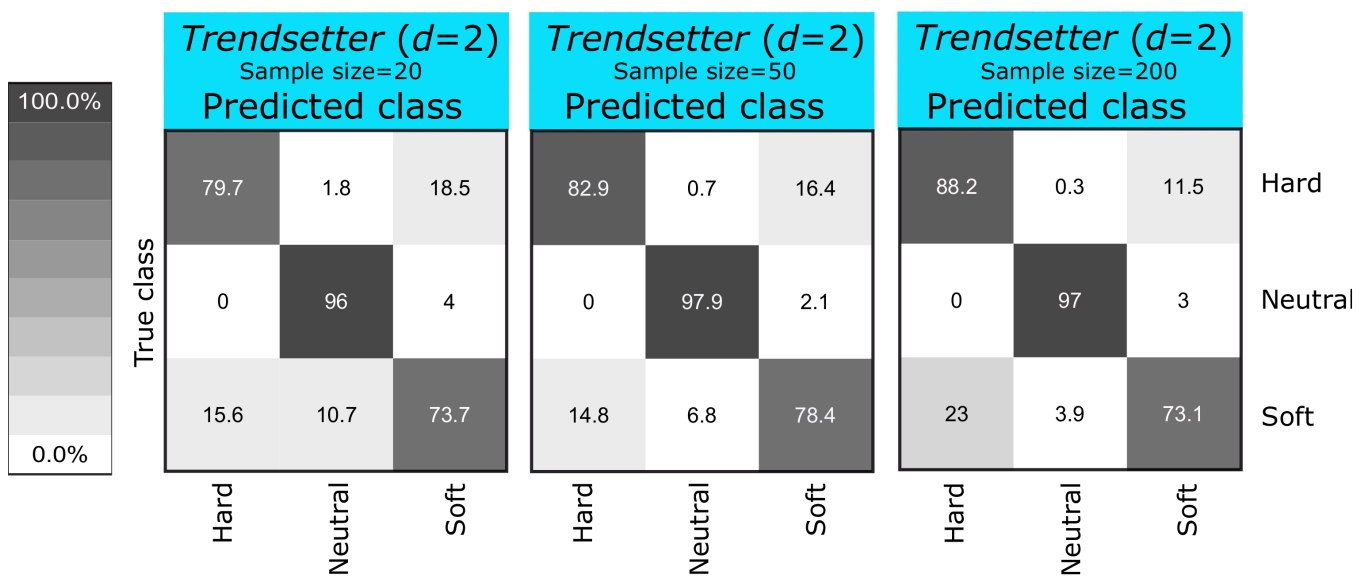


Figure S16: Confusion matrices comparing classification rates of *Trendsetter* with a linear ($d = 2$) trend penalty applied to samples of $n = 20, 50,$ and 200 haplotypes (10, 25, and 100 diploids, respectively). Simulations were performed under a constant-size demographic history and selection coefficients for sweep scenarios drawn uniformly at random on a log scale of $[0.005, 0.5]$. *Trendsetter* was trained with three classes: neutral, hard sweep, and soft sweep.

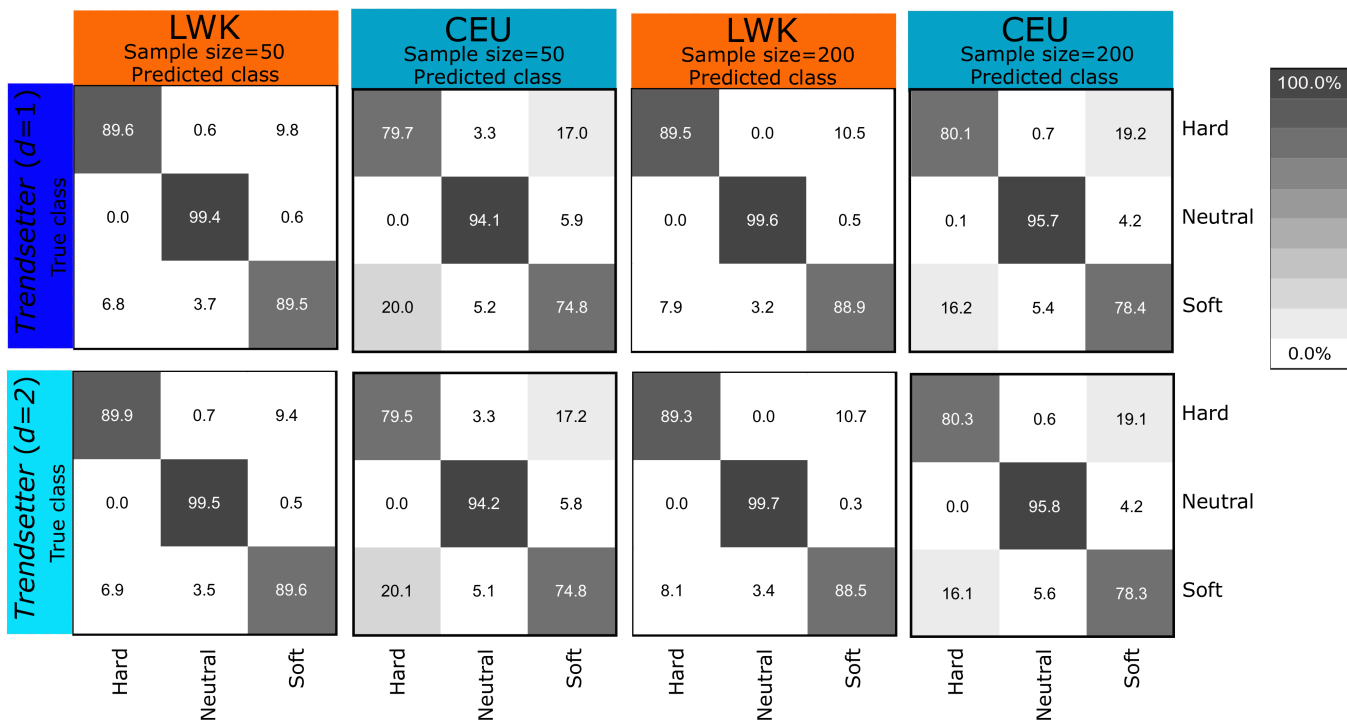


Figure S17: Confusion matrices comparing classification rates of *Trendsetter* with constant ($d = 1$) and linear ($d = 2$) trend penalties applied to samples of $n = 50$ and 200 haplotypes (25 and 100 diploids, respectively). Simulations were performed under demographic specifications for LWK (African) or CEU (European) and selection coefficients for sweep scenarios drawn uniformly at random on a log scale of $[0.005, 0.5]$. *Trendsetter* was trained with three classes: neutral, hard sweep, and soft sweep.

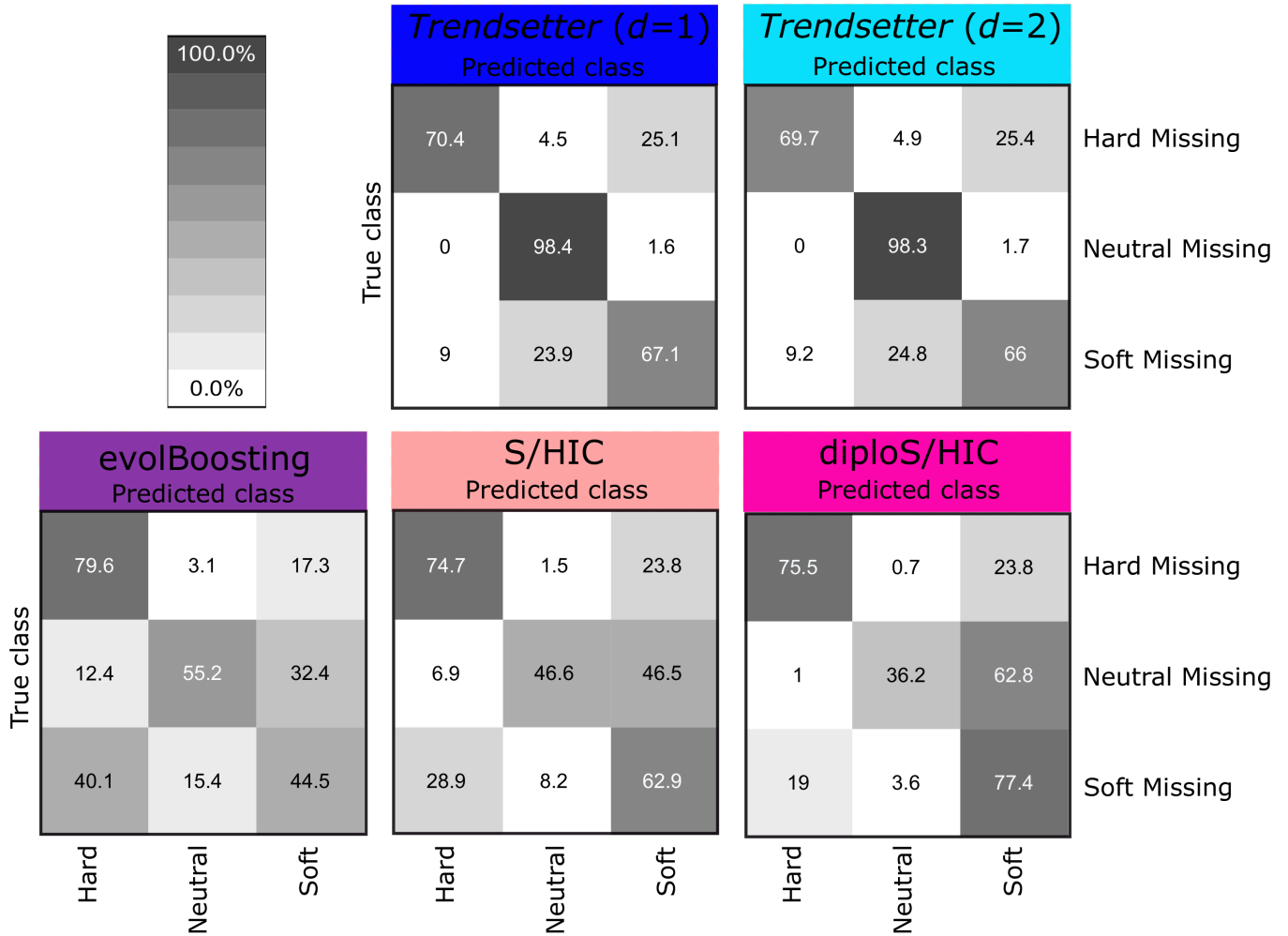


Figure S18: Confusion matrices comparing classification rates of *Trendsetter* with constant ($d = 1$) and linear ($d = 2$) trend penalties, evolBoosting, S/HIC, and diploS/HIC applied to scenarios with missing data. Simulations were performed under a constant-size demographic history and selection coefficients for sweep scenarios drawn uniformly at random on a log scale of $[0.005, 0.5]$. All methods were trained with three classes: neutral, hard sweep, and soft sweep.

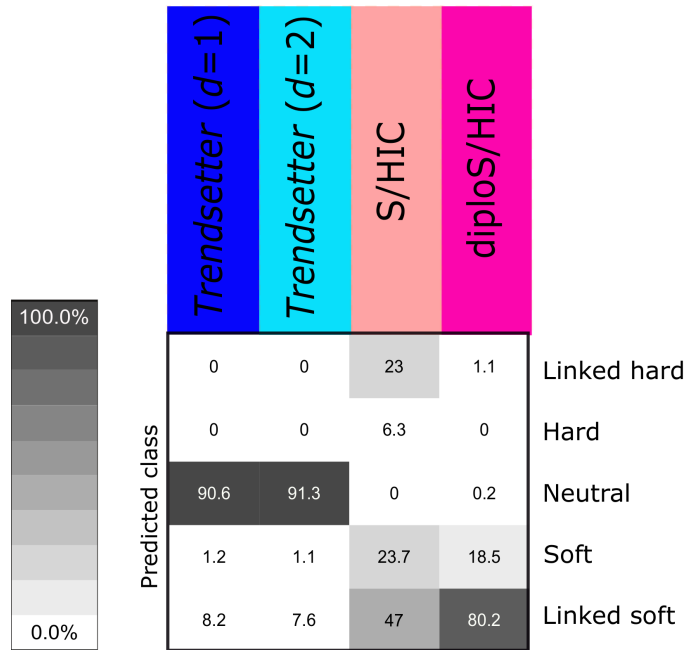


Figure S19: Classification rates of *Trendsetter* with constant ($d = 1$) and linear ($d = 2$) trend penalties, S/HIC, and diploS/HIC applied to neutral regions with missing data when trained with five classes: neutral, hard sweep, soft sweep, linked to hard sweep, and linked to soft sweep. Simulations were performed under a constant-size demographic history and selection coefficients for sweep scenarios drawn uniformly at random on a log scale of $[0.005, 0.5]$.

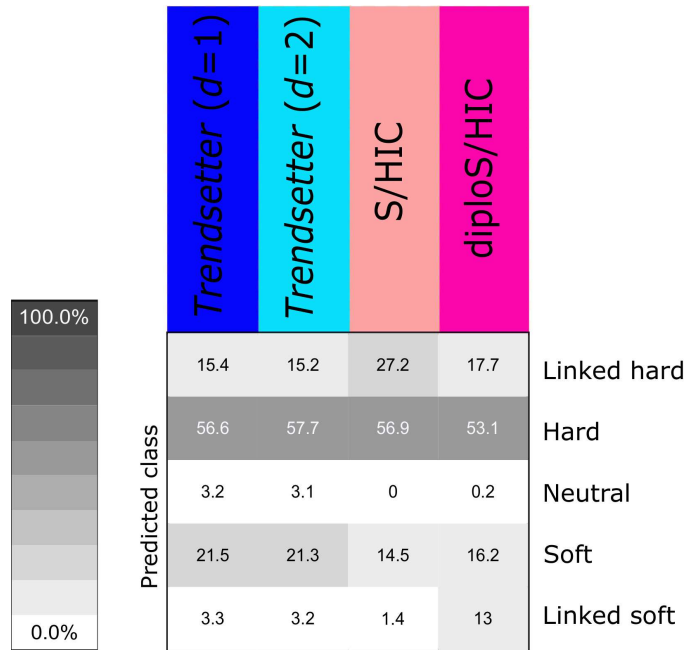


Figure S20: Classification rates of *Trendsetter* with constant ($d = 1$) and linear ($d = 2$) trend penalties, S/HIC, and diploS/HIC applied to hard sweeps with missing data when trained with five classes: neutral, hard sweep, soft sweep, linked to hard sweep, and linked to soft sweep. Simulations were performed under a constant-size demographic history and selection coefficients for sweep scenarios drawn uniformly at random on a log scale of $[0.005, 0.5]$.

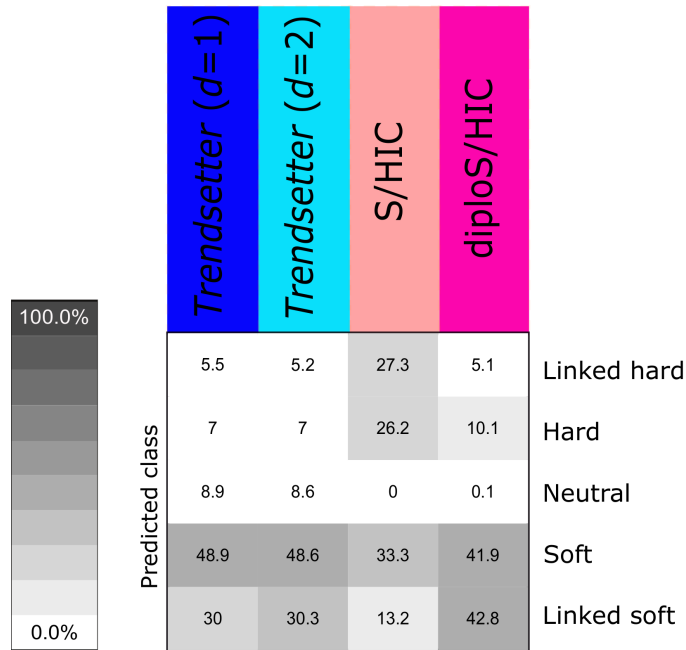


Figure S21: Classification rates of *Trendsetter* with constant ($d = 1$) and linear ($d = 2$) trend penalties, S/HIC, and diploS/HIC applied to soft sweeps with missing data when trained with five classes: neutral, hard sweep, soft sweep, linked to hard sweep, and linked to soft sweep. Simulations were performed under a constant-size demographic history and selection coefficients for sweep scenarios drawn uniformly at random on a log scale of $[0.005, 0.5]$.

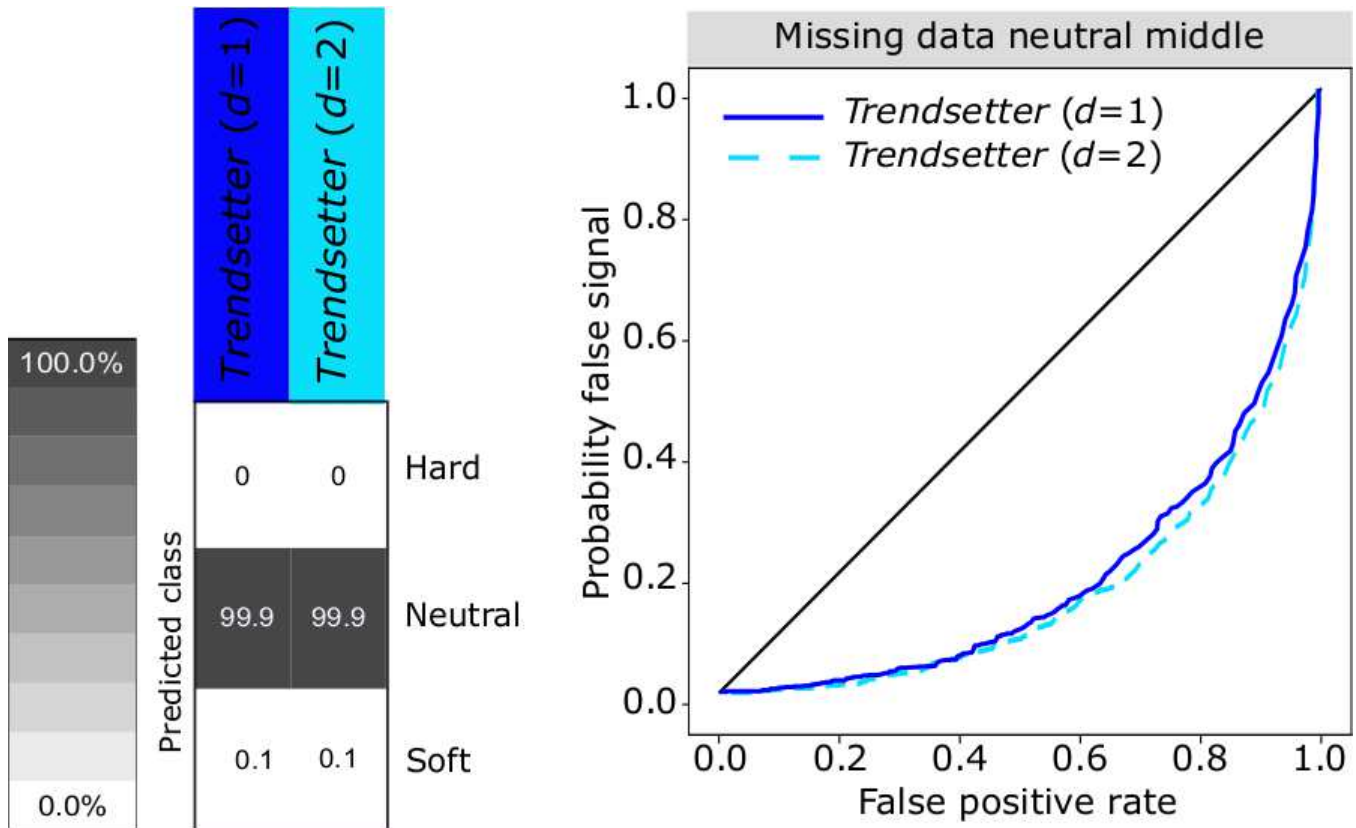


Figure S22: Robustness of mis-classifying neutral genomic regions with extensive missing data in the center of each simulated replicate as a sweep for *Trendsetter* with constant ($d = 1$) and linear ($d = 2$) trend penalties, under a constant-size demographic history. (Left) Classification rates for neutrally-evolving regions with extensive missing data in their centers. (Right) Probability of mis-classifying neutrally-evolving regions with extensive missing data in their centers as a sweep, by comparing the probability of any sweep (hard or soft) under simulations with missing data (probability of false signal) to the same probability under neutral simulations (false positive rate). *Trendsetter* was trained with three classes: neutral, hard sweep, and soft sweep, with selection coefficients for sweep scenarios drawn uniformly at random on a log scale of $[0.005, 0.5]$.

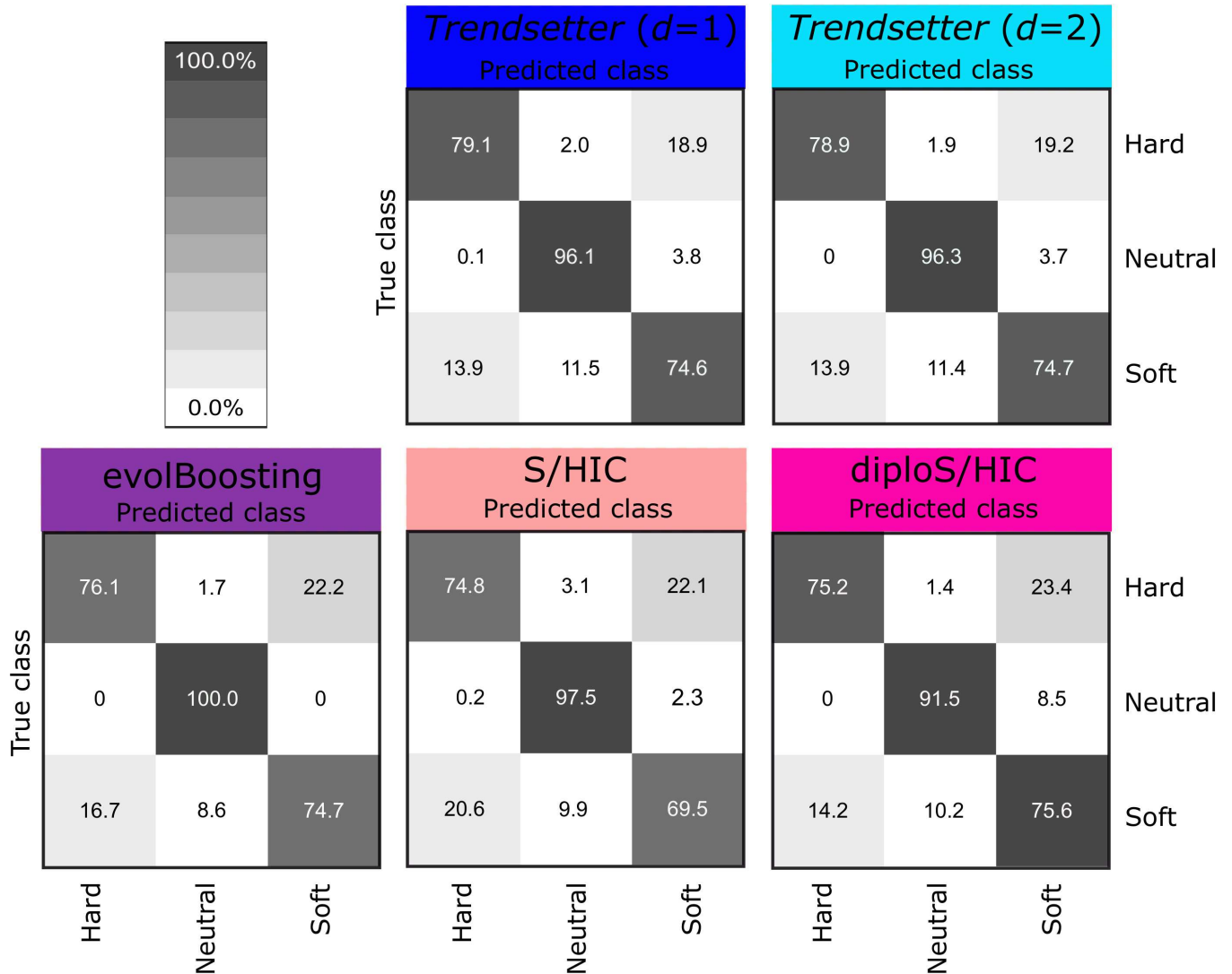


Figure S23: Confusion matrices comparing classification rates of *Trendsetter* with constant ($d = 1$) and linear ($d = 2$) trend penalties, evolBoosting, S/HIC, and diploS/HIC trained with simulations containing missing data and applied to scenarios with missing data. Simulations were performed under a constant-size demographic history and selection coefficients for sweep scenarios drawn uniformly at random on a log scale of $[0.005, 0.5]$. All methods were trained with three classes: neutral, hard sweep, and soft sweep.

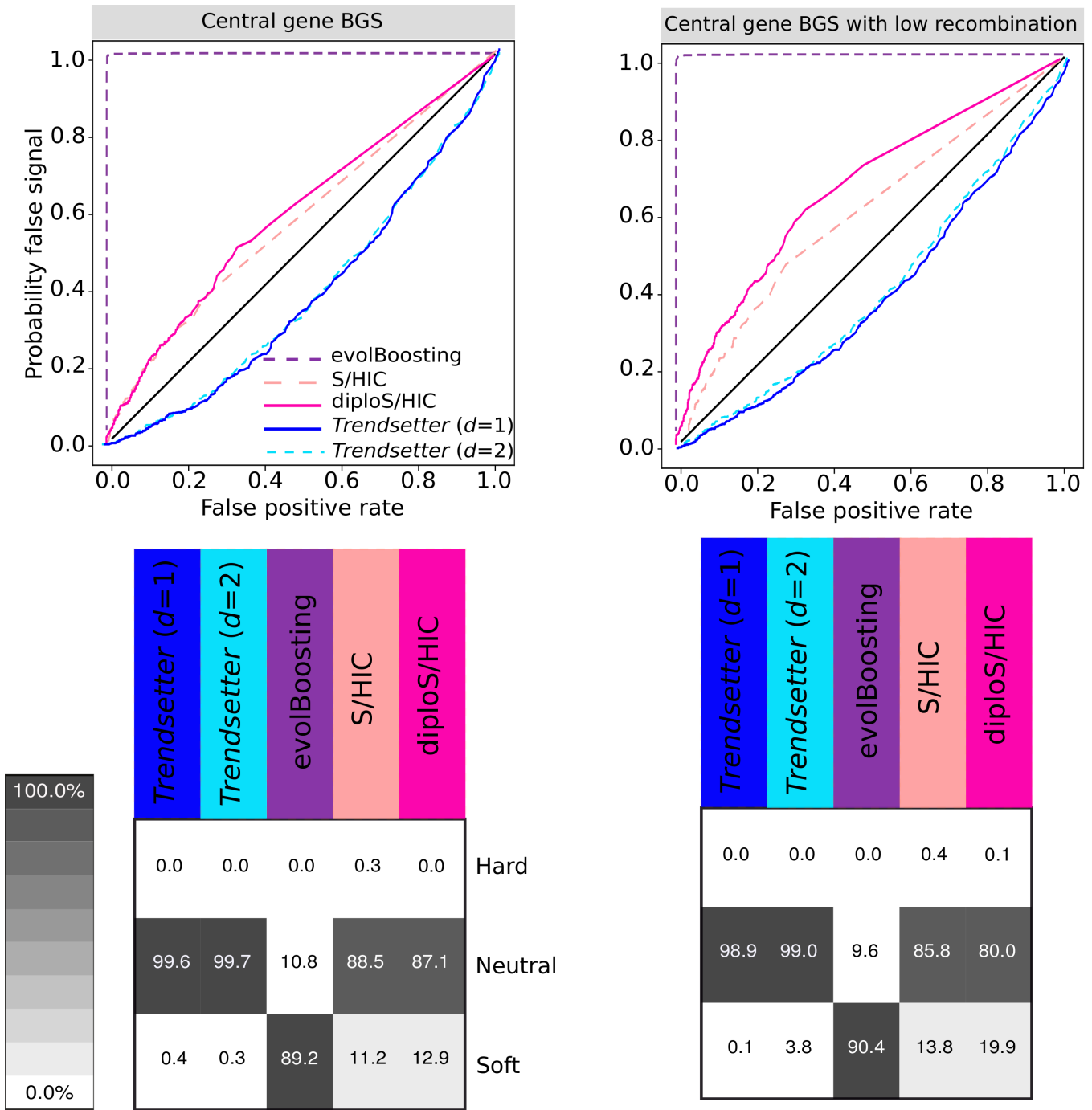


Figure S24: Robustness of mis-classifying genomic regions undergoing background selection for various methods, under a constant-size demographic history and a centrally-located protein-coding gene in which strongly-deleterious alleles continuously arise (see *Materials and methods*). (Left) Classification rates for and probability of mis-classifying regions evolving under background selection with a centrally-located genic region. (Right) Classification rates for and probability of mis-classifying regions evolving under background selection with a centrally-located genic region and 100-fold decrease in recombination rate within the genic region. (Top) Probability of mis-classifying regions evolving under background selection, by comparing the combined probability of any sweep (hard or soft) under simulations with background selection (probability of false signal) to the same probability under neutral simulations (false positive rate). All methods were trained with three classes: neutral, hard sweep, and soft sweep, with selection coefficients for sweep scenarios drawn uniformly at random on a log scale of $[0.005, 0.5]$.

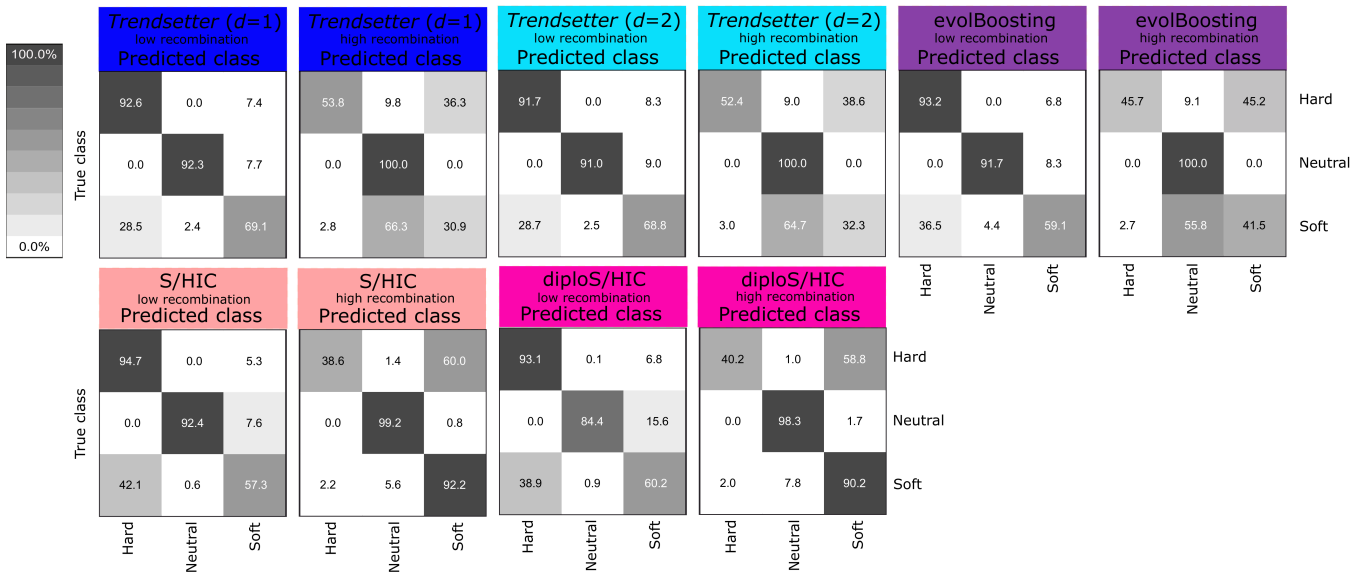


Figure S25: Confusion matrices comparing classification rates of *Trendsetter* with constant ($d = 1$) and linear ($d = 2$) trend penalties, evolBoosting, S/HIC, and diploS/HIC under recombination rate misspecification. Test simulation recombination rates were either $r = 5 \times 10^{-9}$ (low recombination) or $r = 5 \times 10^{-8}$ (high recombination). Simulations were performed under a constant-size demographic history. All methods were trained with three classes: neutral, hard sweep, and soft sweep, with selection coefficients for sweep scenarios drawn uniformly at random on a log scale of $[0.005, 0.5]$, with uniform recombination rate of $r = 10^{-8}$.

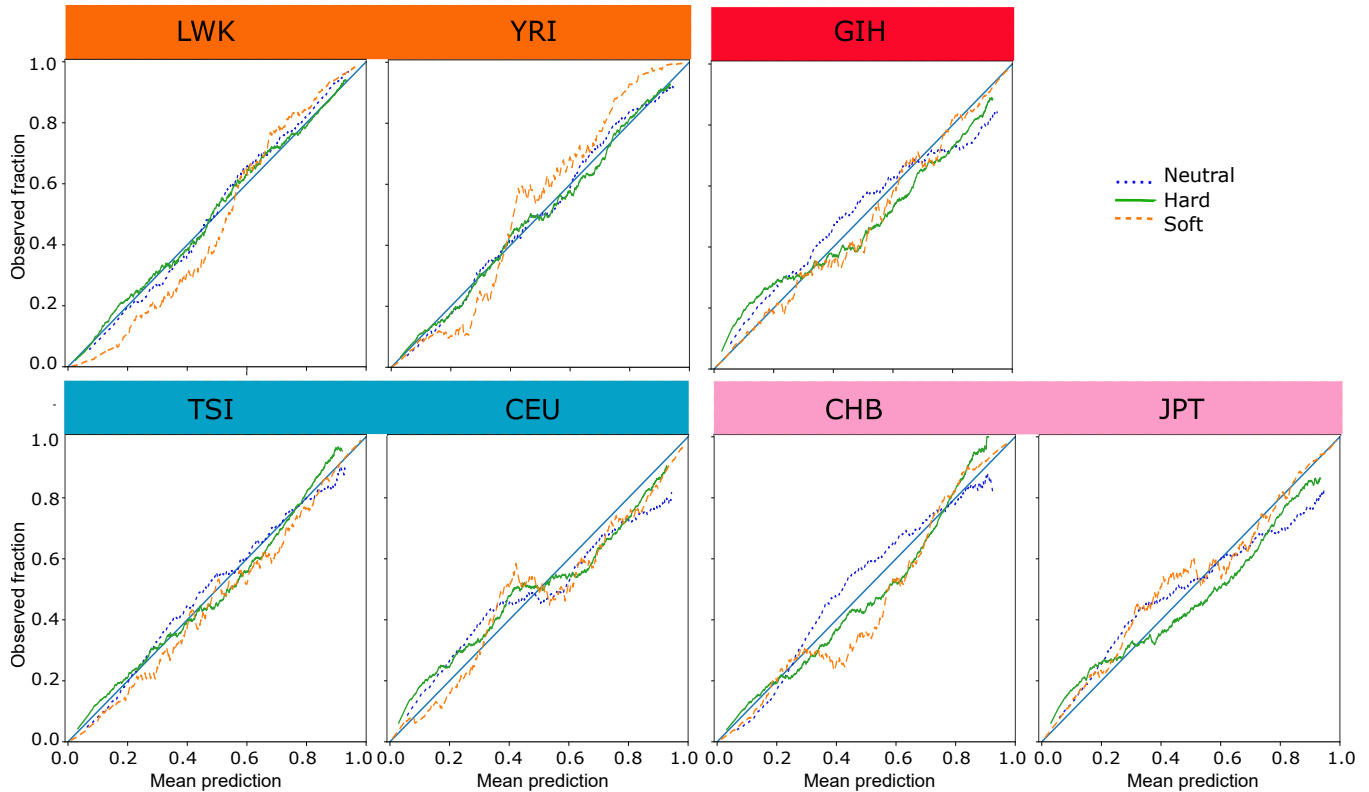


Figure S26: Reliability curves for each of three classes (neutral, hard sweep, and soft sweep) for *Trendsetter* with a linear ($d = 2$) trend penalty trained on data simulated under demographic parameters estimated (Terhorst et al., 2017) from African (LWK and YRI), South Asian (GIH), European (TSI and CEU), and East Asian (CHB and JPT) populations. For each class we calculate the proportion of observed instances with probability for that class falling within bins of width 0.05 in sliding windows with increments of 0.001 from 0.0 to 1.0, with the first window centered at 0.025 and the last at 0.975.

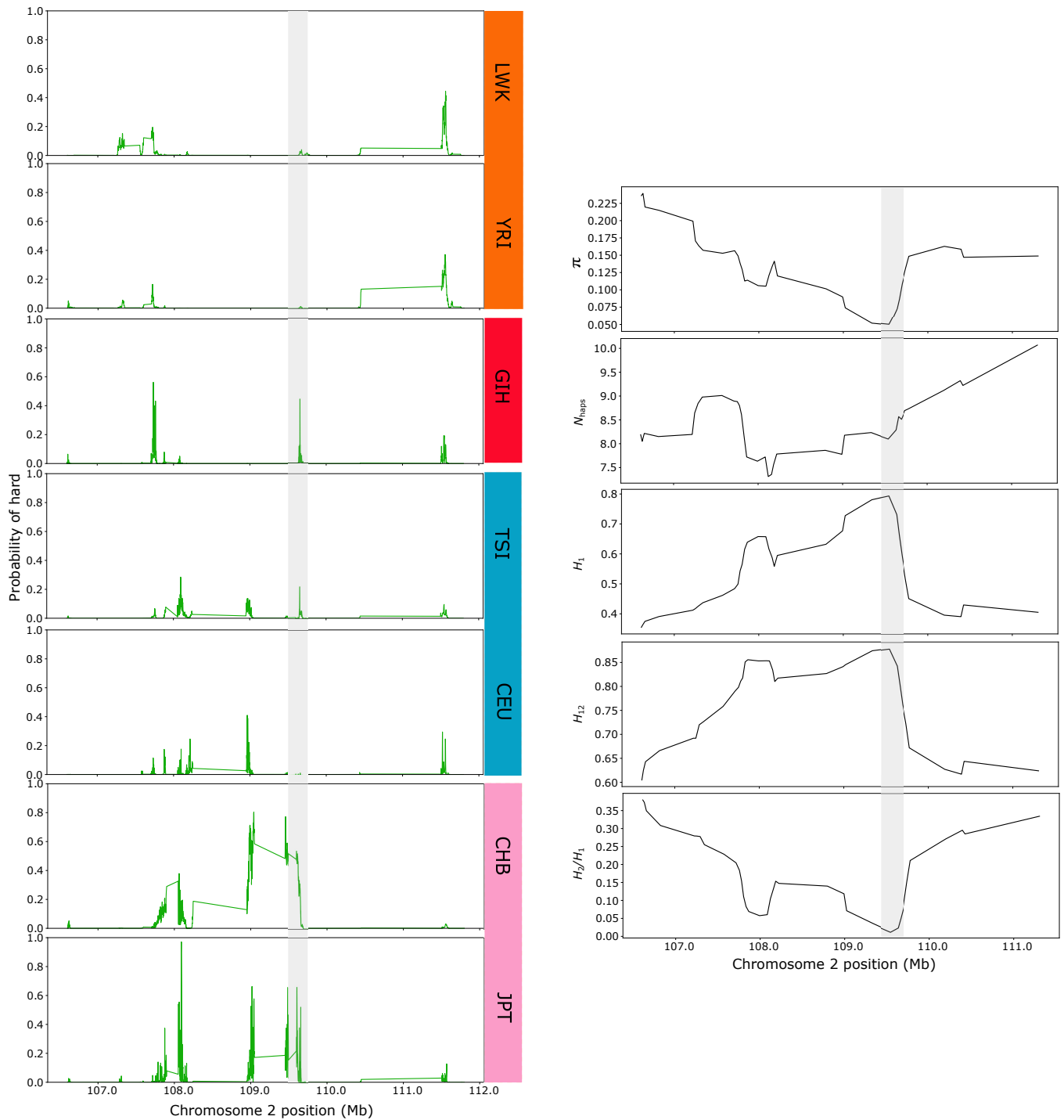


Figure S27: Patterns of a selective sweep across the region on chromosome 2 surrounding the *EDAR* gene in African (LWK and YRI), South Asian (GIH), European (TSI and CEU), and East Asian (CHB and JPT) populations. (Left) Probabilities of a hard sweep using *Trendsetter* with a linear ($d = 2$) trend penalty. (Right) Distributions of summary statistics employed by *Trendsetter* across the region on chromosome 2 surrounding the *EDAR* gene in the Han Chinese (CHB) population. The distribution for each statistic is based on the mean of 30 contiguous data points that were used as input to *Trendsetter* as described in *Materials and Methods* in a sliding window, shifting by one data point. The gray bar represents the location of *EDAR*.

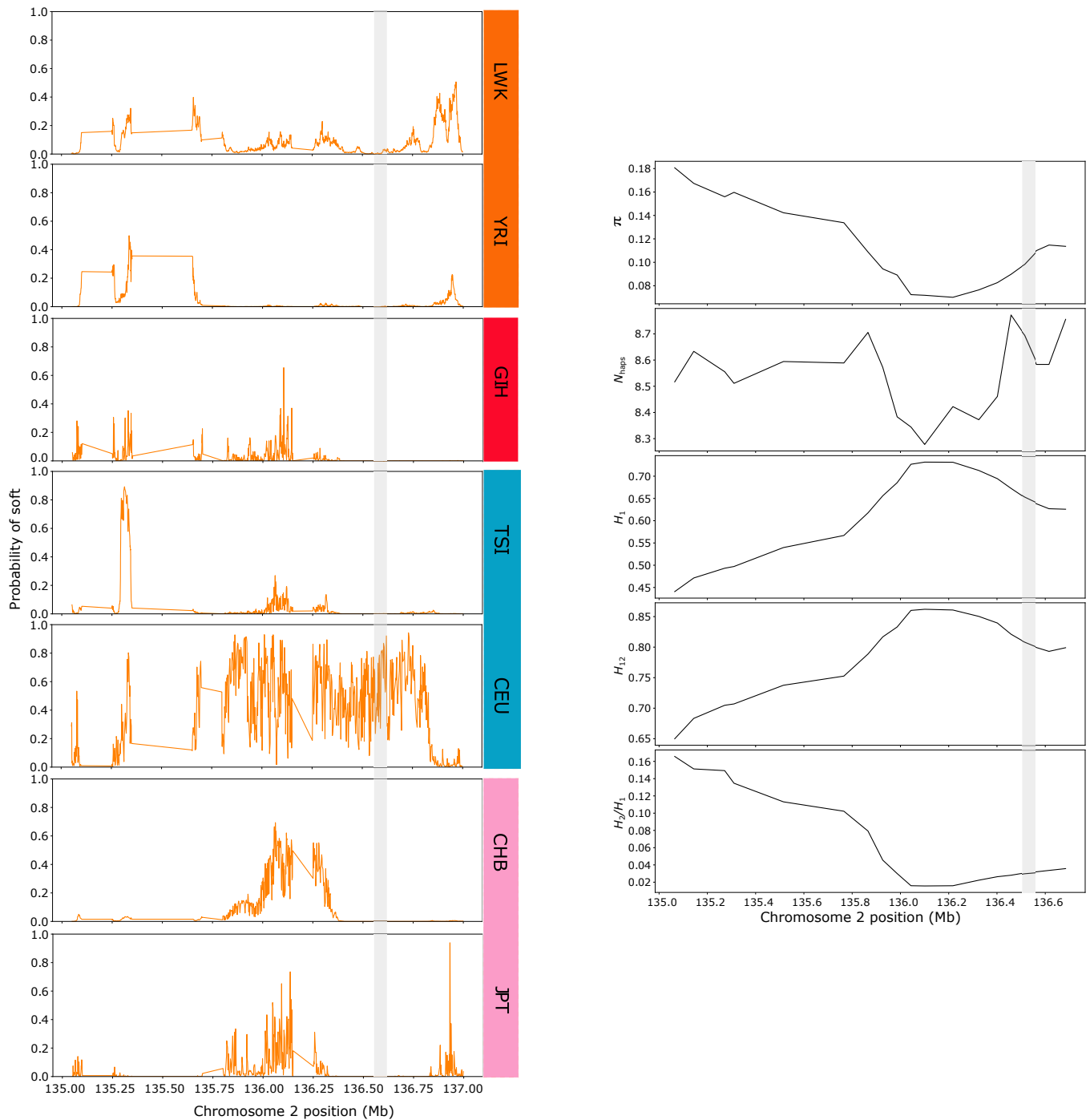


Figure S28: Patterns of a selective sweep across the region on chromosome 2 surrounding the *LCT* gene in African (LWK and YRI), South Asian (GIH), European (TSI and CEU), and East Asian (CHB and JPT) populations. (Left) Probabilities of a soft sweep using *Trendsetter* with a linear ($d = 2$) trend penalty. (Right) Distributions of summary statistics employed by *Trendsetter* across the region on chromosome 2 surrounding the *LCT* gene in the European from Utah (CEU) population. The distribution for each statistic is based on the mean of 30 contiguous data points that were used as input to *Trendsetter* as described in *Materials and Methods* in a sliding window, shifting by one data point. The gray bar represents the location of *LCT*.

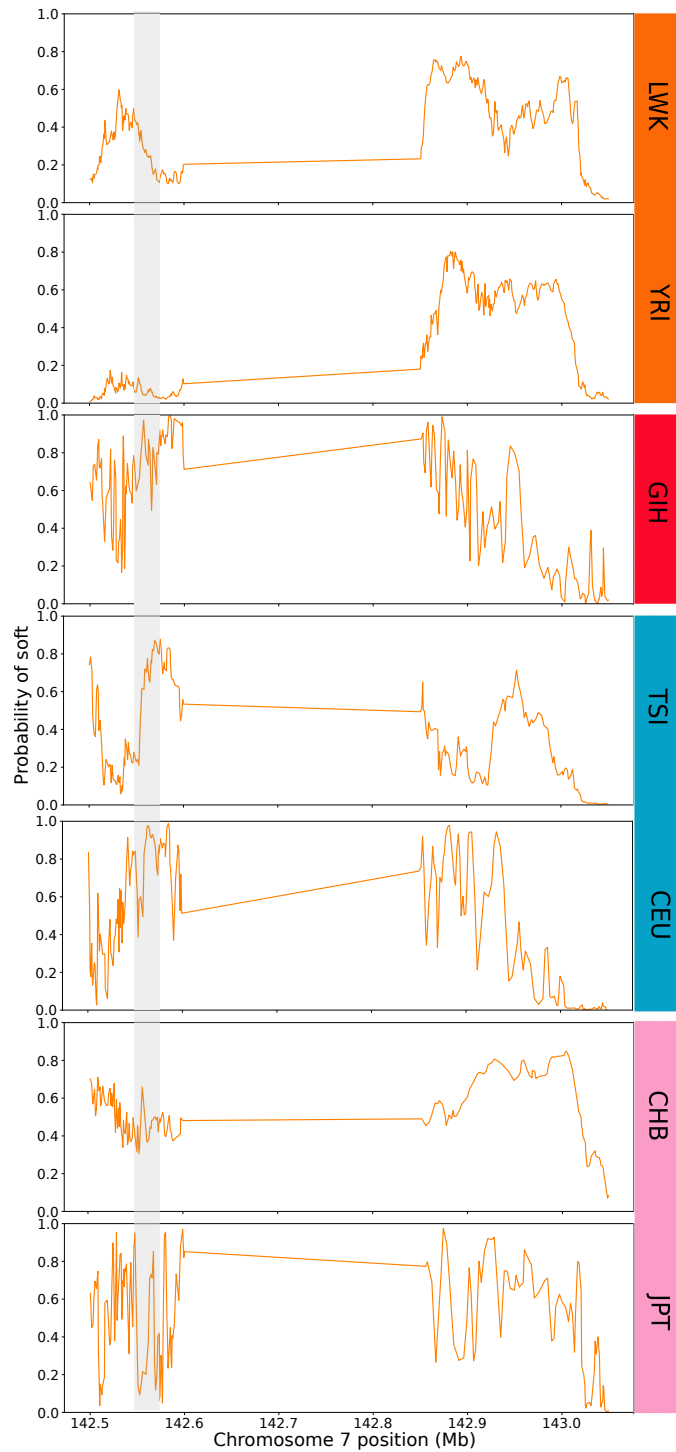


Figure S29: Patterns of a selective sweep across the region on chromosome 7 surrounding the *TRVP6* gene in African (LWK and YRI), South Asian (GIH), European (TSI and CEU), and East Asian (CHB and JPT) populations. Probabilities of a soft sweep using *Trendsetter* with a linear ($d = 2$) trend penalty across the region on chromosome 7 surrounding the *TRVP6* gene. The gray bar represents the location of *TRVP6*.

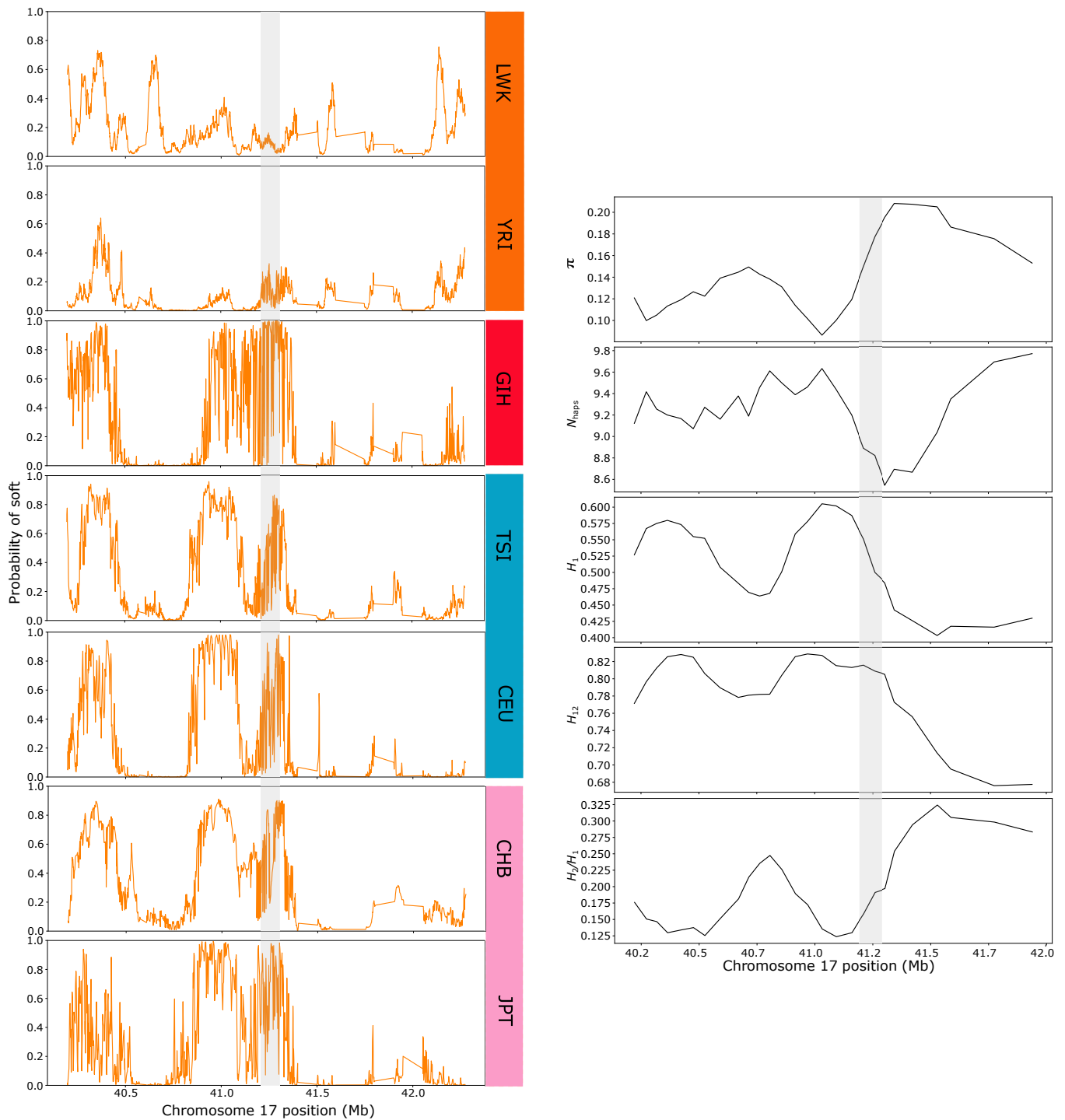


Figure S30: Patterns of a selective sweep across the region on chromosome 17 surrounding the *BRCA1* gene in African (LWK and YRI), South Asian (GIH), European (TSI and CEU), and East Asian (CHB and JPT) populations. (Left) Probabilities of a soft sweep using *Trendsetter* with a linear ($d = 2$) trend penalty. (Right) Distributions of summary statistics employed by *Trendsetter* across the region on chromosome 17 surrounding the *BRCA1* gene in the Han Chinese (CHB) population. The distribution for each statistic is based on the mean of 30 contiguous data points that were used as input to *Trendsetter* as described in *Materials and Methods* in a sliding window, shifting by one data point. The gray bar represents the location of *BRCA1*.

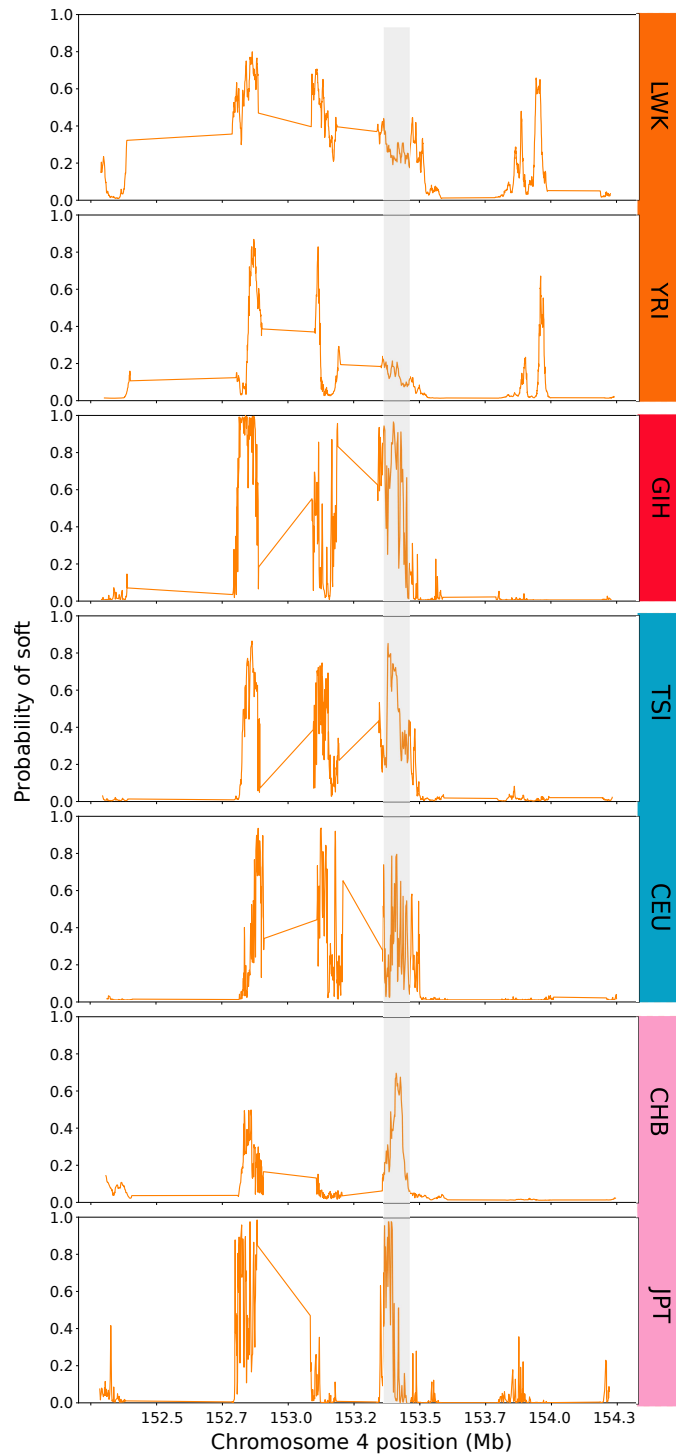


Figure S31: Patterns of a selective sweep across the region on chromosome 4 surrounding the *FBXW7* gene in African (LWK and YRI), South Asian (GIH), European (TSI and CEU), and East Asian (CHB and JPT) populations. Probabilities of a soft sweep using *Trendsetter* with a linear ($d = 2$) trend penalty across the region on chromosome 7 surrounding the *FBXW7* gene. The gray bar represents the location of *FBXW7*.



Figure S32: Heatmap representing the sharing of hard sweep classifications across worldwide human populations. The cell at row j and column k represents the proportion of non-overlapping 10 kb genomic segments classified as a hard sweep in the population at row j that are also classified as a hard sweep in the population at column k . By definition, this heatmap is asymmetric. Note that the range of values in this heatmap is bounded between 0.8 and 1.0 because large fractions of hard sweeps are shared between populations.

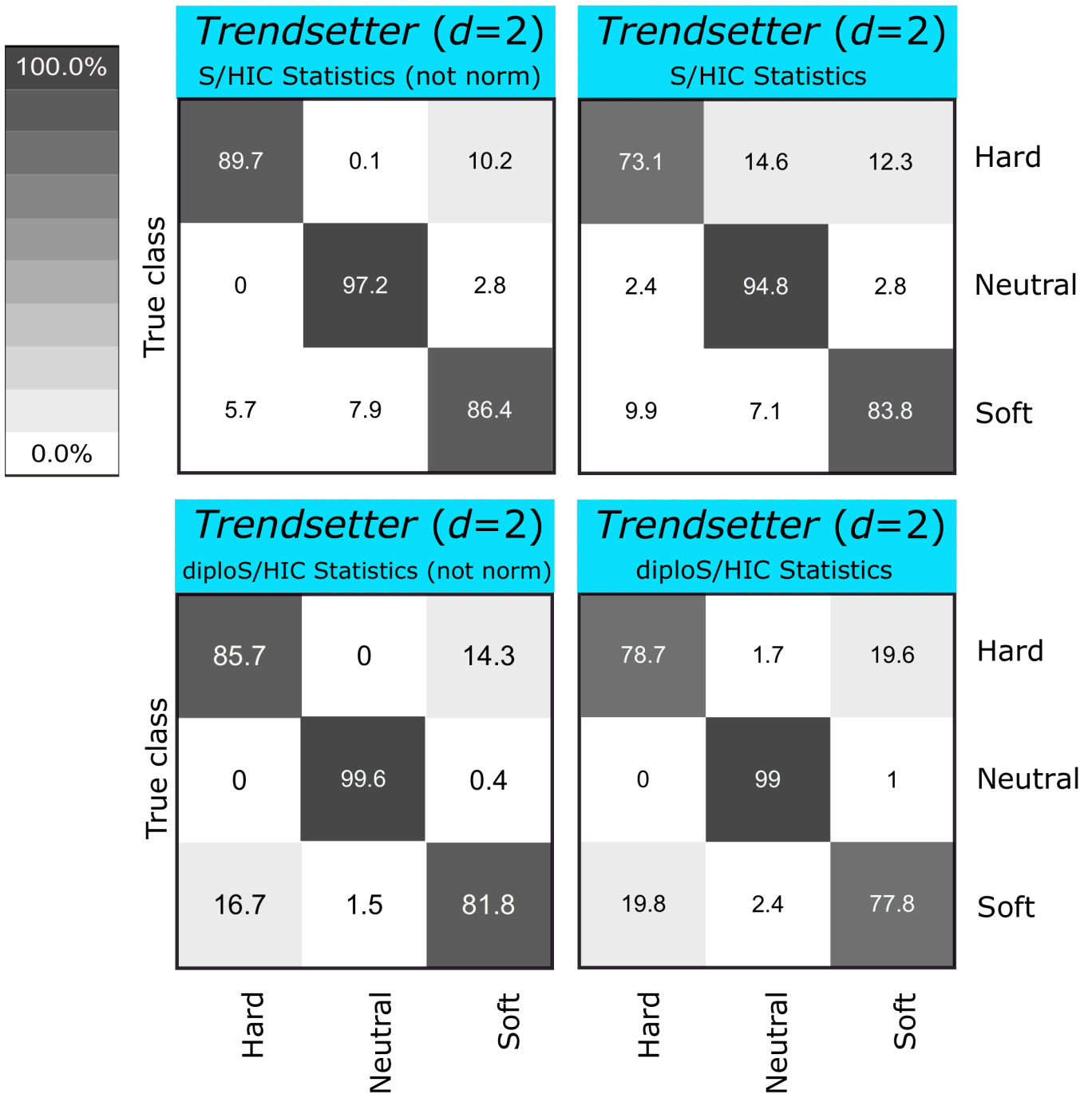


Figure S33: Confusion matrices comparing classification rates of *Trendsetter* with a linear ($d = 2$) trend penalty applied to summary statistics computed by S/HIC and diploS/HIC (both normalized and non-normalized). S/HIC and diploS/HIC by default use summary statistics that have normalized such that each summary statistic is a value between 0 and 1, and that the summation of values of a summary statistic across the set of windows that it is calculated is 1. Simulations were performed under a constant-size demographic history and selection coefficients for sweep scenarios drawn uniformly at random on a log scale of $[0.005, 0.5]$. All methods were trained with three classes: neutral, hard sweep, and soft sweep.

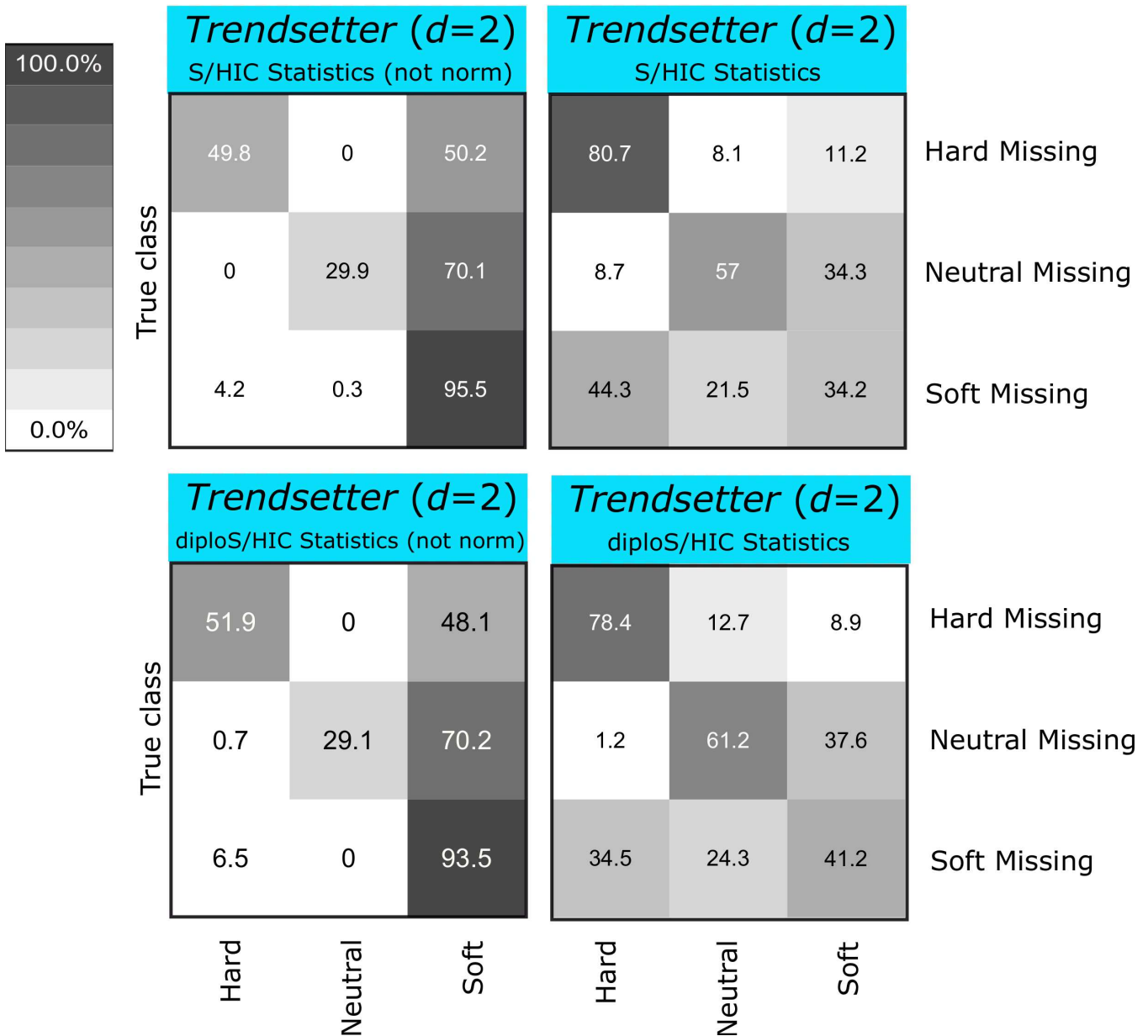


Figure S34: Confusion matrices comparing classification rates of *Trendsetter* with a linear ($d = 2$) trend penalty applied to summary statistics computed by S/HIC and diploS/HIC (both normalized and non-normalized) in the presence of missing data. S/HIC and diploS/HIC by default use summary statistics that are normalized such that each summary statistic is a value between 0 and 1, and that the summation of values of a summary statistic across the set of windows that it is calculated is 1. Simulations were performed under a constant-size demographic history and selection coefficients for sweep scenarios drawn uniformly at random on a log scale of $[0.005, 0.5]$. All methods were trained with three classes: neutral, hard sweep, and soft sweep.

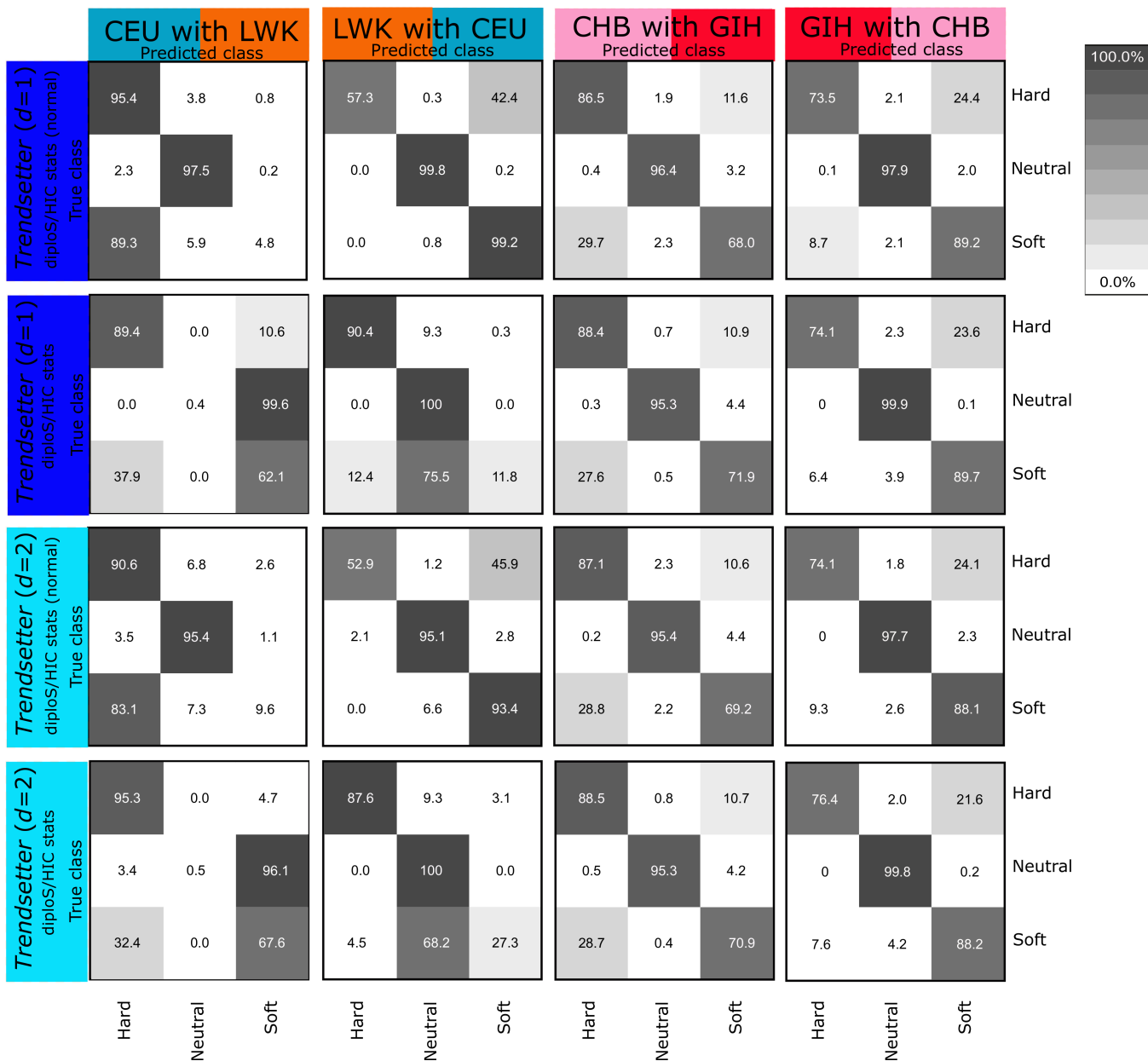


Figure S35: Confusion matrices comparing classification rates of *Trendsetter* with constant ($d = 1$) and linear ($d = 2$) trend penalties under demographic mis-specification (*i.e.*, testing on a population history that is different from the one that was used to train the classifier) when employing summary statistics computed by diploS/HIC (both normalized and non-normalized). The column label indicates the test population followed by the training population. All methods were trained with three classes: neutral, hard sweep, and soft sweep, with selection coefficients for sweep scenarios drawn uniformly at random on a log scale of $[0.005, 0.5]$.

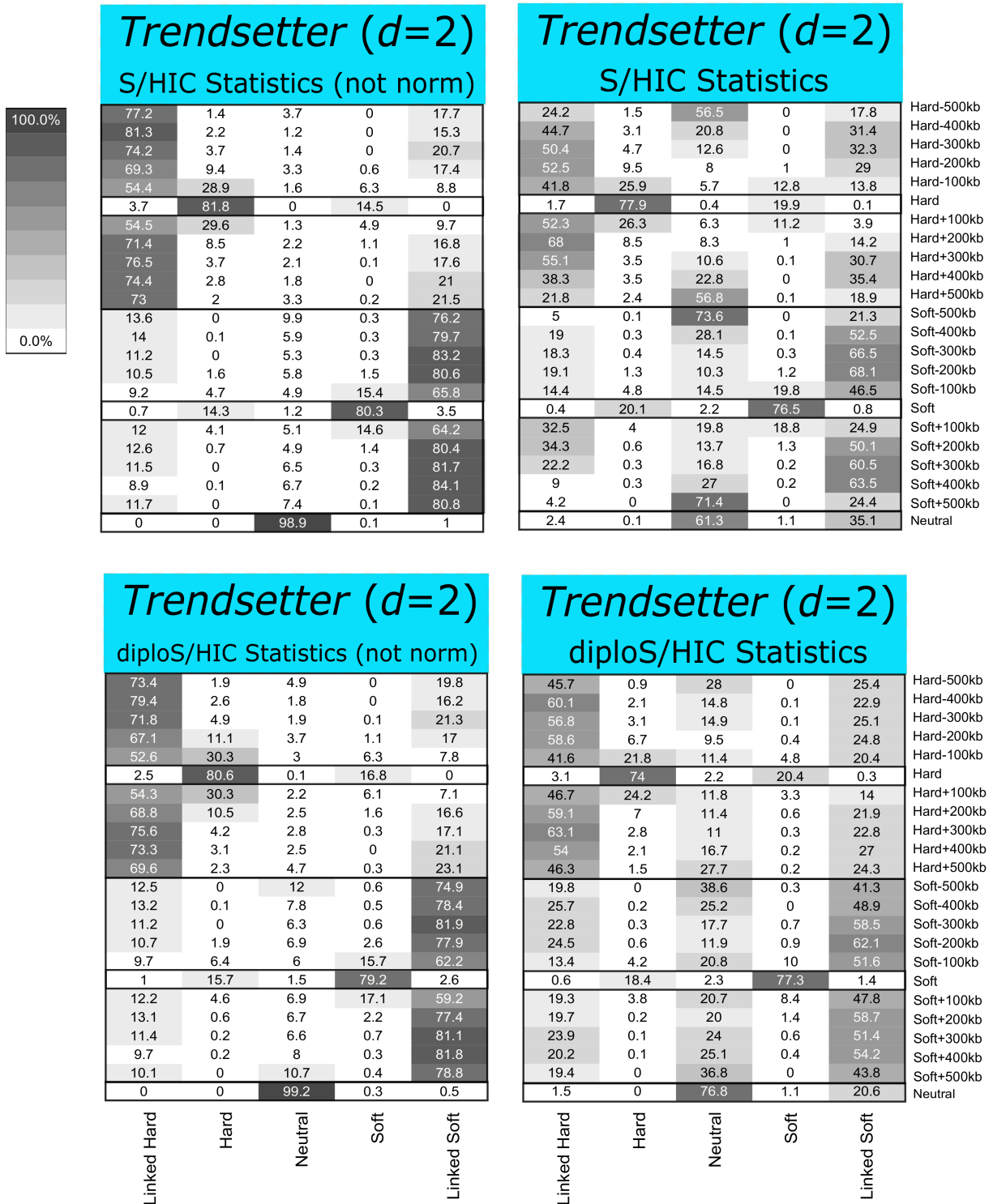


Figure S36: Confusion matrices comparing classification rates of *Trendsetter* with a linear ($d = 2$) trend penalty applied to summary statistics computed by S/HIC (both normalized and non-normalized) and diploS/HIC. S/HIC and diploS/HIC by default use summary statistics that are normalized such that each summary statistic is a value between 0 and 1, and that the summation of values of a summary statistic across the set of windows that it is calculated is 1. Simulations were performed under a constant-size demographic history and selection coefficients for sweep scenarios drawn uniformly at random on a log scale of $[0.005, 0.5]$. All methods were trained with five classes: neutral, hard sweep, soft sweep, linked to hard sweep, and linked to soft sweep.

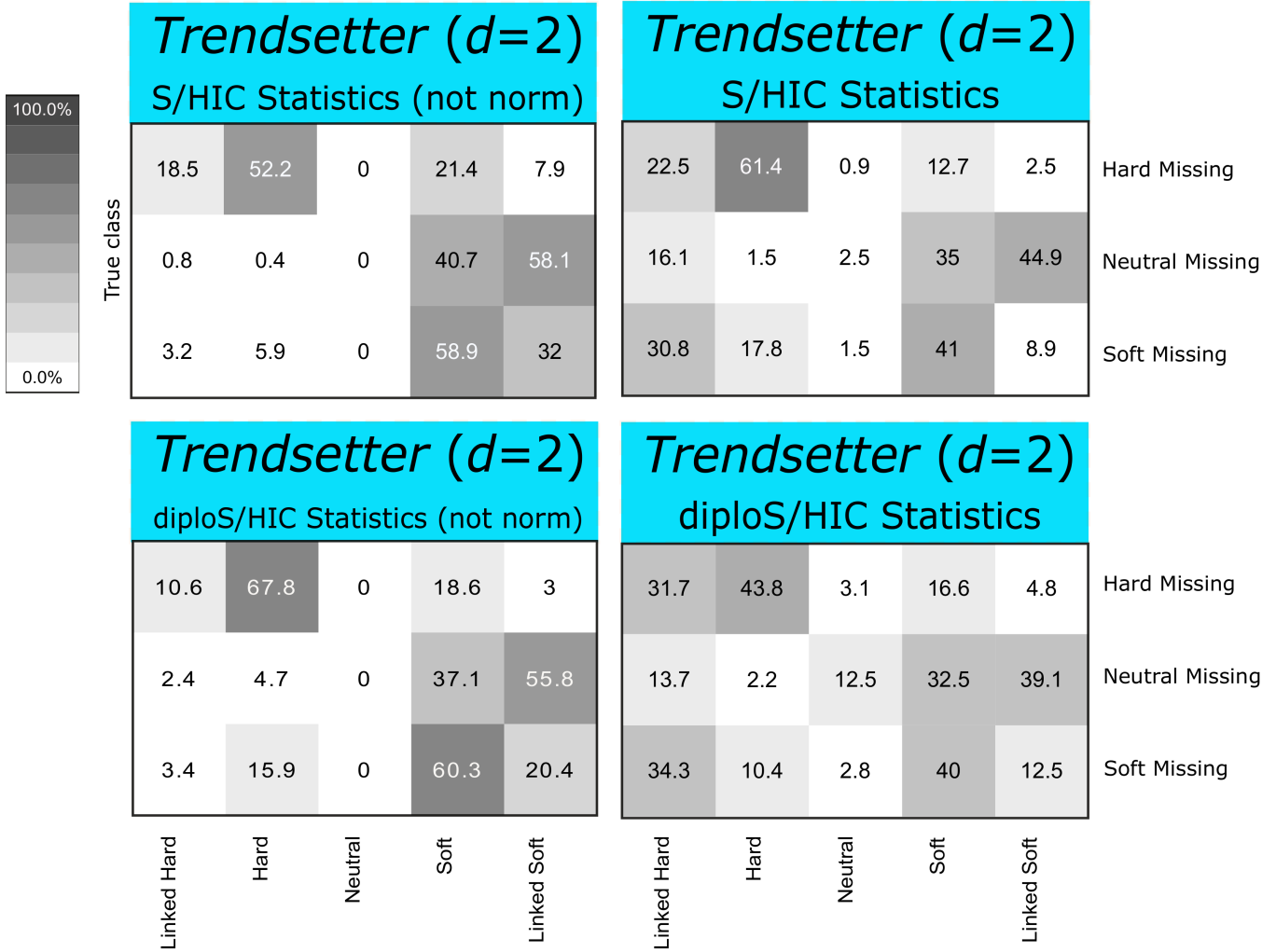


Figure S37: Confusion matrices comparing classification rates of *Trendsetter* with a linear ($d = 2$) trend penalty applied to summary statistics computed by S/HIC (both normalized and non-normalized) and diploS/HIC in the presence of missing data. S/HIC and diploS/HIC by default use summary statistics that are normalized such that each summary statistic is a value between 0 and 1, and that the summation of values of a summary statistic across the set of windows that it is calculated is 1. Simulations were performed under a constant-size demographic history and selection coefficients for sweep scenarios drawn uniformly at random on a log scale of $[0.005, 0.5]$. All methods were trained with five classes: neutral, hard sweep, soft sweep, linked to hard sweep, and linked to soft sweep.

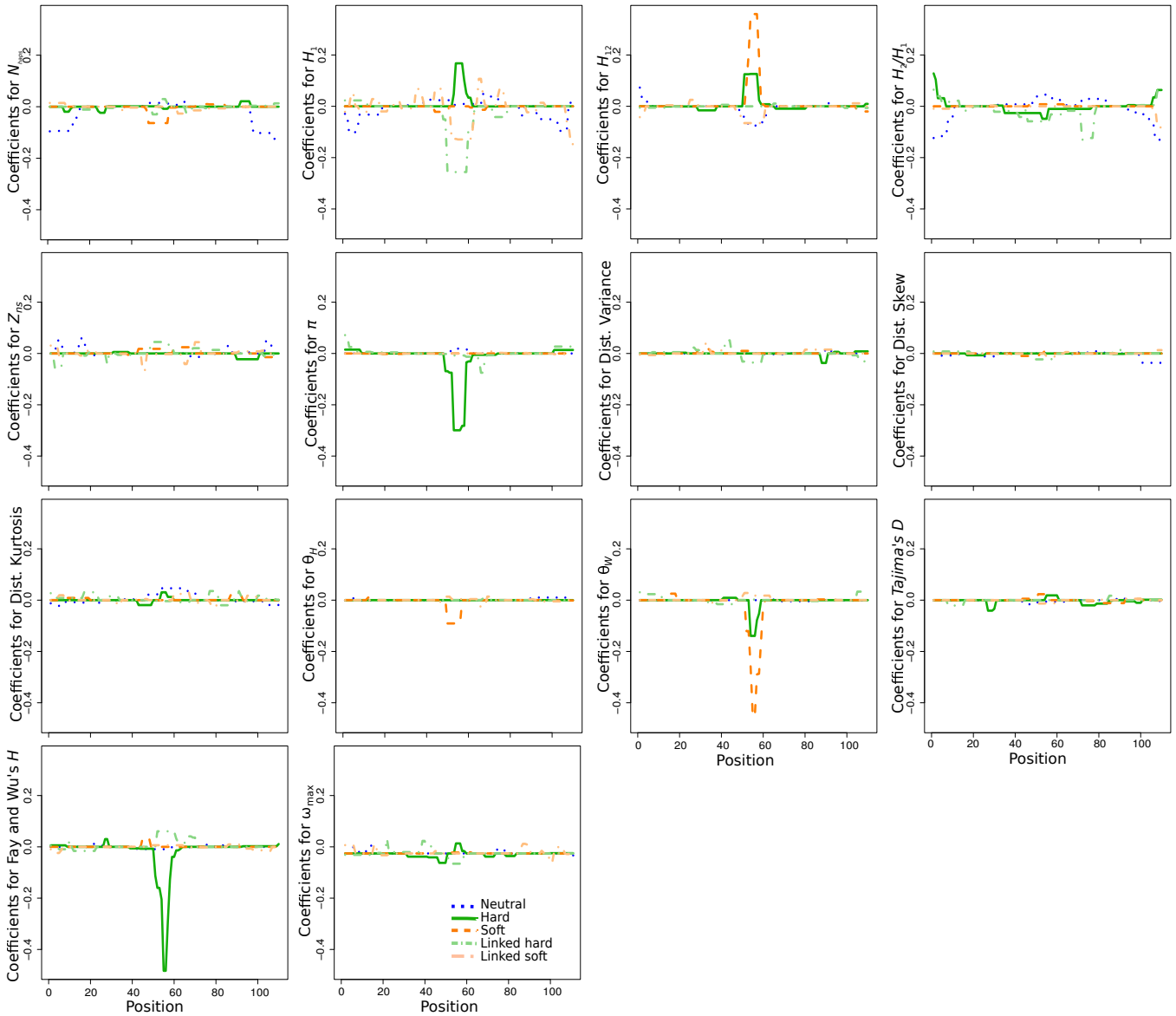


Figure S38: Spatial distributions of regression coefficients (β s) in neutral, hard sweep, soft sweep, linked to hard sweep, and linked to soft sweep scenarios for summary statistics N_{haps} , H_1 , H_{12} , H_2/H_1 , Z_{ns} , $\hat{\pi}$, variance, skewness, and kurtosis of the number of differences between pairs of haplotypes, θ_H , θ_W , Tajima's D , Fay and Wu's H , and ω_{max} for *Trendsetter* applied with a constant ($d = 1$) trend penalty. *Trendsetter* was trained on simulations with selection strength $s \in [0.005, 0.5]$ sampled uniformly at random on a log scale. Note that the distributions of regression coefficients for all summary statistics are plotted on the same scale, thereby making the distributions of some summaries difficult to decipher as their magnitudes are relatively small.

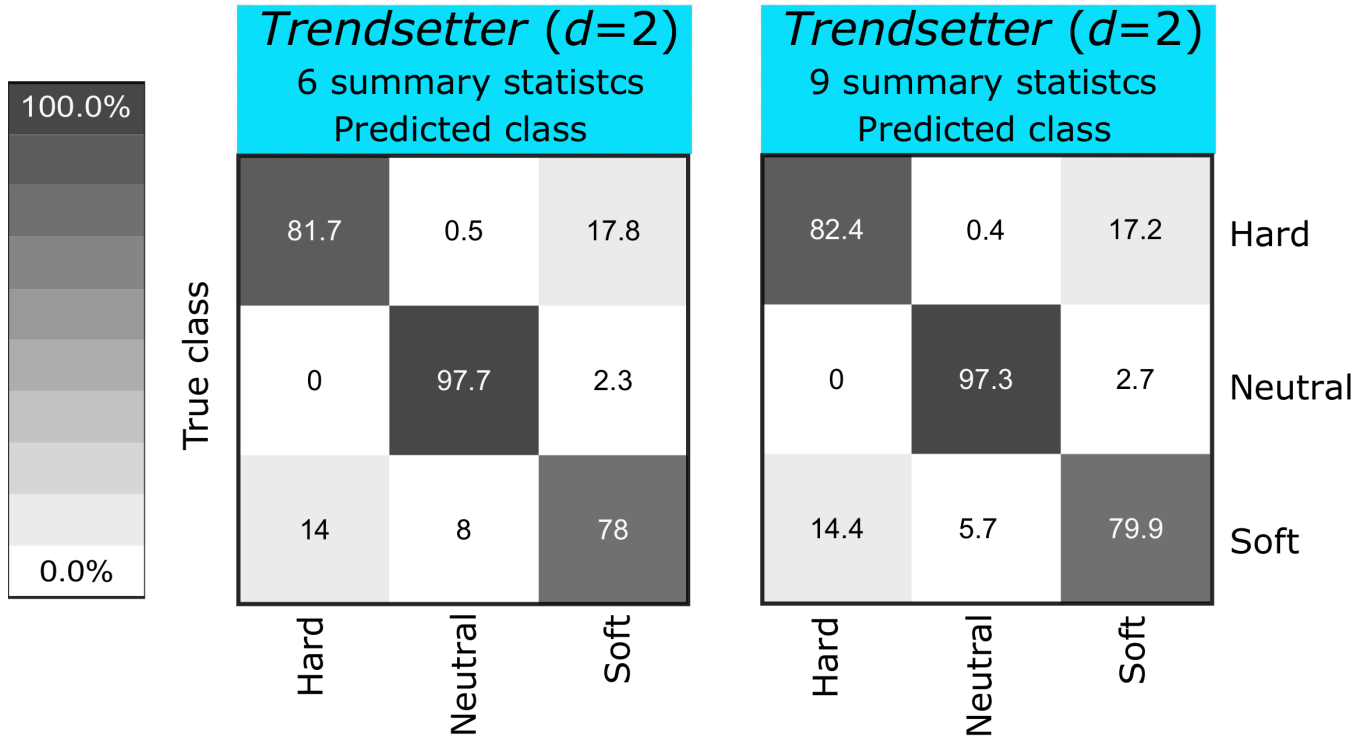


Figure S39: Confusion matrices showing classification rates of *Trendsetter* with a linear ($d = 2$) trend penalty applied to samples of multilocus genotype data. (Left) Classification rates when using summary statistics $\hat{\pi}$, HR^2 , N_{geno} , G_1 , G_{123} , and G_2/G_1 . (Right) Classification rates when using the variance, skewness, and kurtosis of the distributions of pairwise differences between multilocus genotypes in addition to the six statistics used in the left panel. Simulations for both results were performed under a constant-size demographic history and selection coefficients for sweep scenarios drawn uniformly at random on a log scale of $[0.005, 0.5]$. *Trendsetter* was trained with three classes: neutral, hard sweep, and soft sweep.

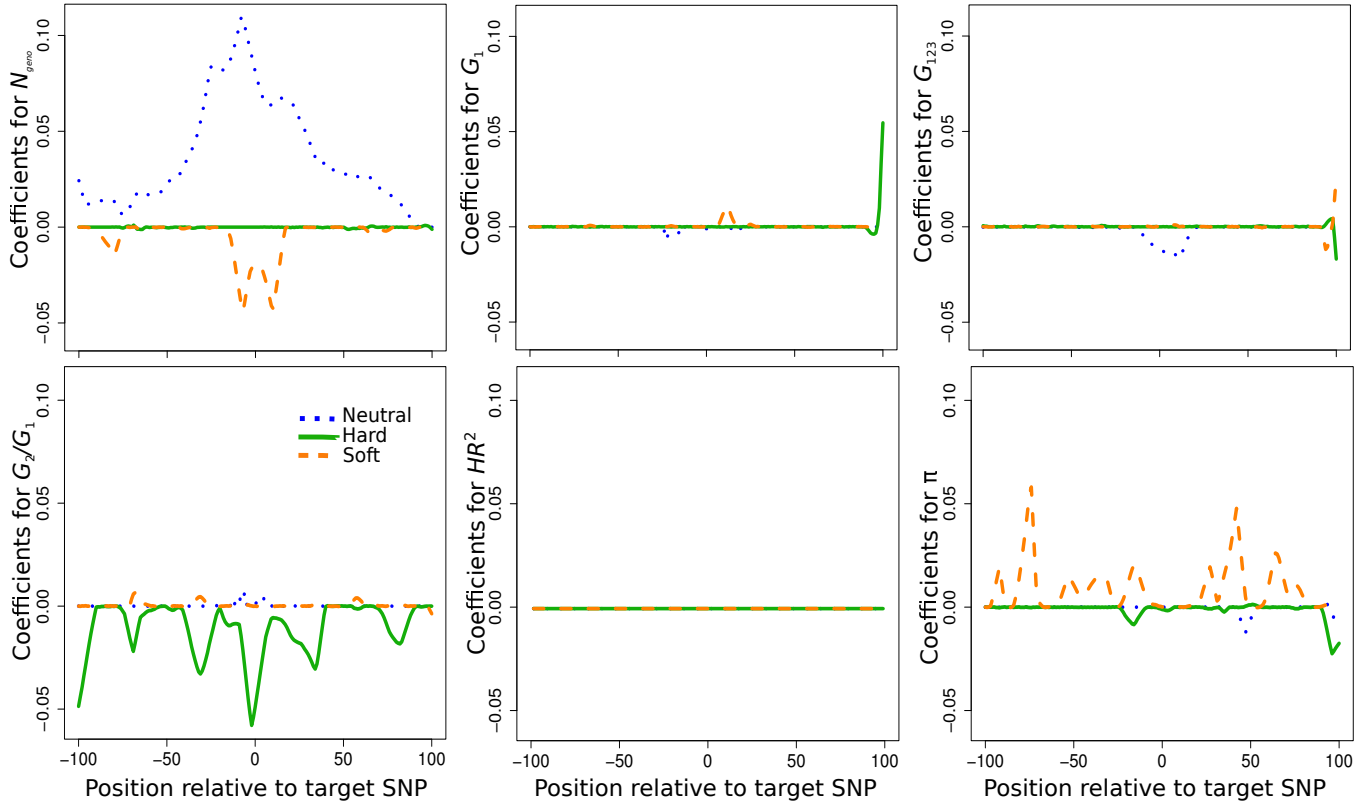


Figure S40: Spatial distributions of regression coefficients (β s) in neutral, hard sweep, and soft sweep scenarios for summary statistics N_{geno} , G_1 , G_{123} , G_2/G_1 , HR^2 , and $\hat{\pi}$. *Trendsetter* applied with a linear ($d = 2$) trend penalty. *Trendsetter* was trained on simulations with selection strength $s \in [0.005, 0.5]$ sampled uniformly at random on a log scale. Note that the distributions of regression coefficients for all summary statistics are plotted on the same scale, thereby making the distributions of some summaries difficult to decipher as their magnitudes are relatively small.

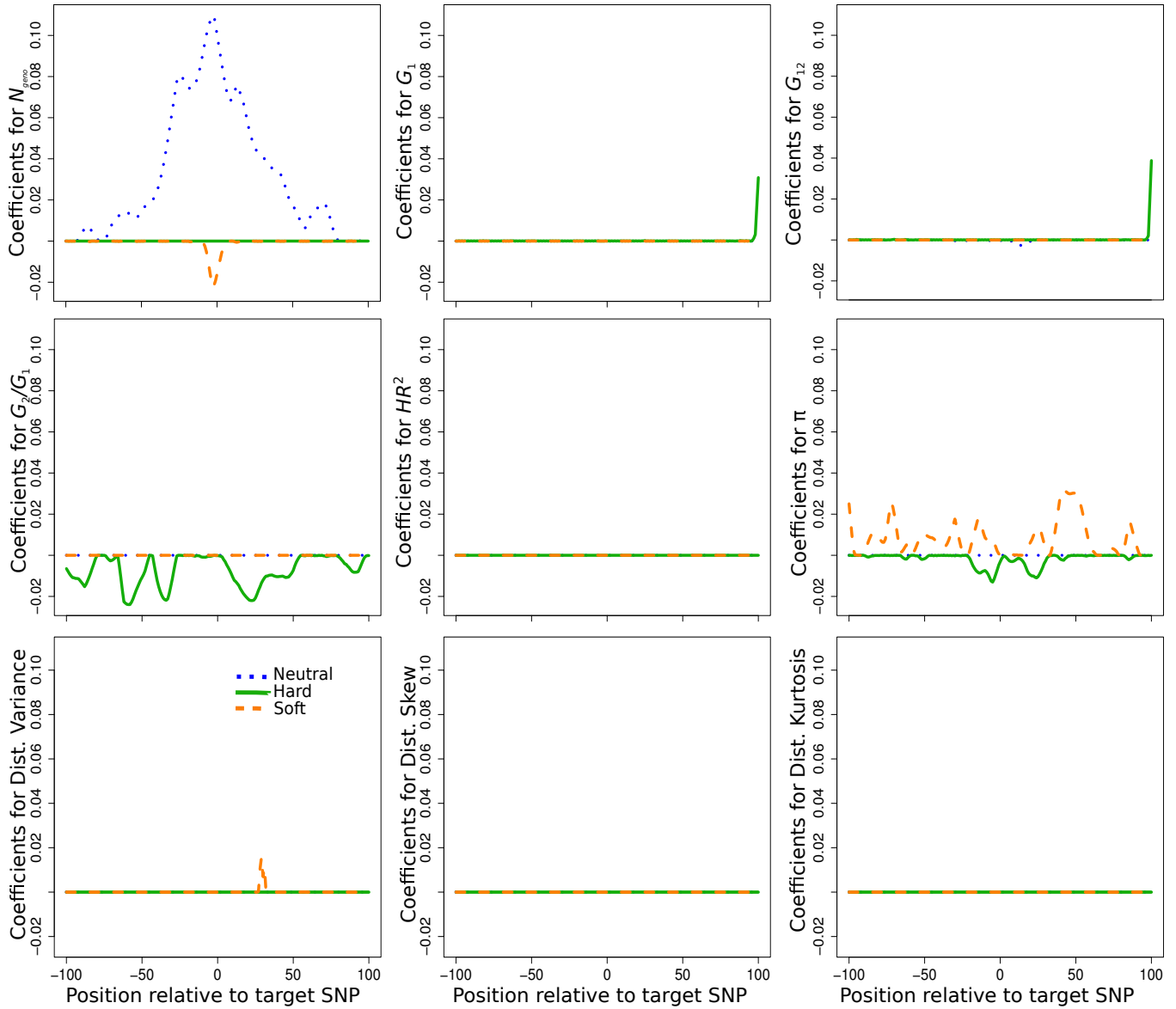


Figure S41: Spatial distributions of regression coefficients (β_s) in neutral, hard sweep, and soft sweep scenarios for summary statistics N_{geno} , G_1 , G_{123} , G_2/G_1 , HR^2 , $\hat{\pi}$, and the variance, skewness, and kurtosis of the distribution of pairwise differences of the sample for *Trendsetter* applied with a linear ($d = 2$) trend penalty. *Trendsetter* was trained on simulations with selection strength $s \in [0.005, 0.5]$ sampled uniformly at random on a log scale. Note that the distributions of regression coefficients for all summary statistics are plotted on the same scale, thereby making the distributions of some summaries difficult to decipher as their magnitudes are relatively small.

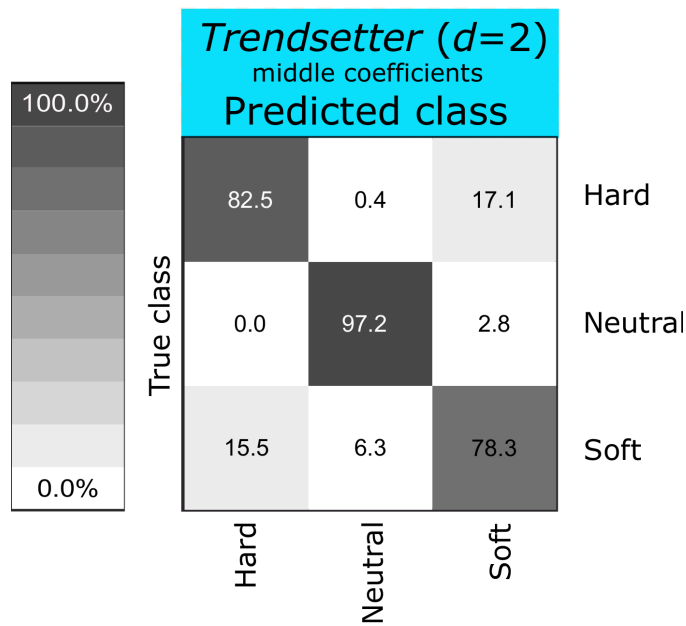


Figure S42: Confusion matrix showing classification rates of *Trendsetter* with a linear ($d = 2$) trend penalty in which only the middle 191 values for each summary statistic along with associated regression coefficients are used when applying *Trendsetter* to test data. All simulations were performed under a constant-size demographic history with selection coefficients for sweep scenarios drawn uniformly at random on a log scale of $[0.005, 0.5]$. *Trendsetter* was trained with three classes: neutral, hard sweep, and soft sweep.

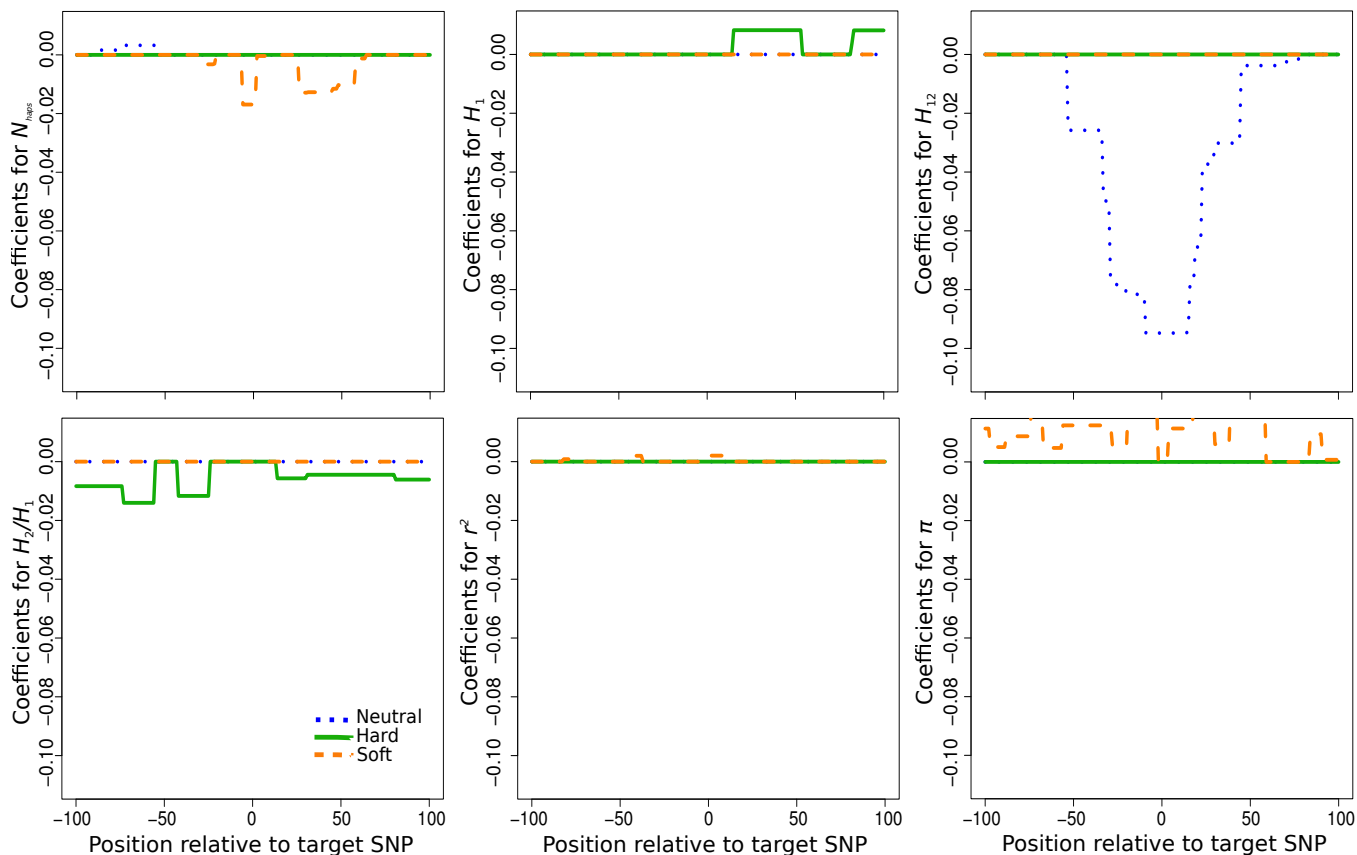


Figure S43: Spatial distributions of regression coefficients (β s) in neutral, hard sweep, and soft sweep scenarios for summary statistics N_{haps} , H_1 , H_{12} , H_2/H_1 , r^2 , and $\hat{\pi}$, for *Trendsetter* applied with a constant ($d = 1$) trend penalty. *Trendsetter* was trained on simulations with selection strength $s \in [0.005, 0.5]$ sampled uniformly at random on a logs for all summary statistics are plotted on the same scale, thereby making the distributions of some summaries difficult to decipher as their magnitudes are relatively small.

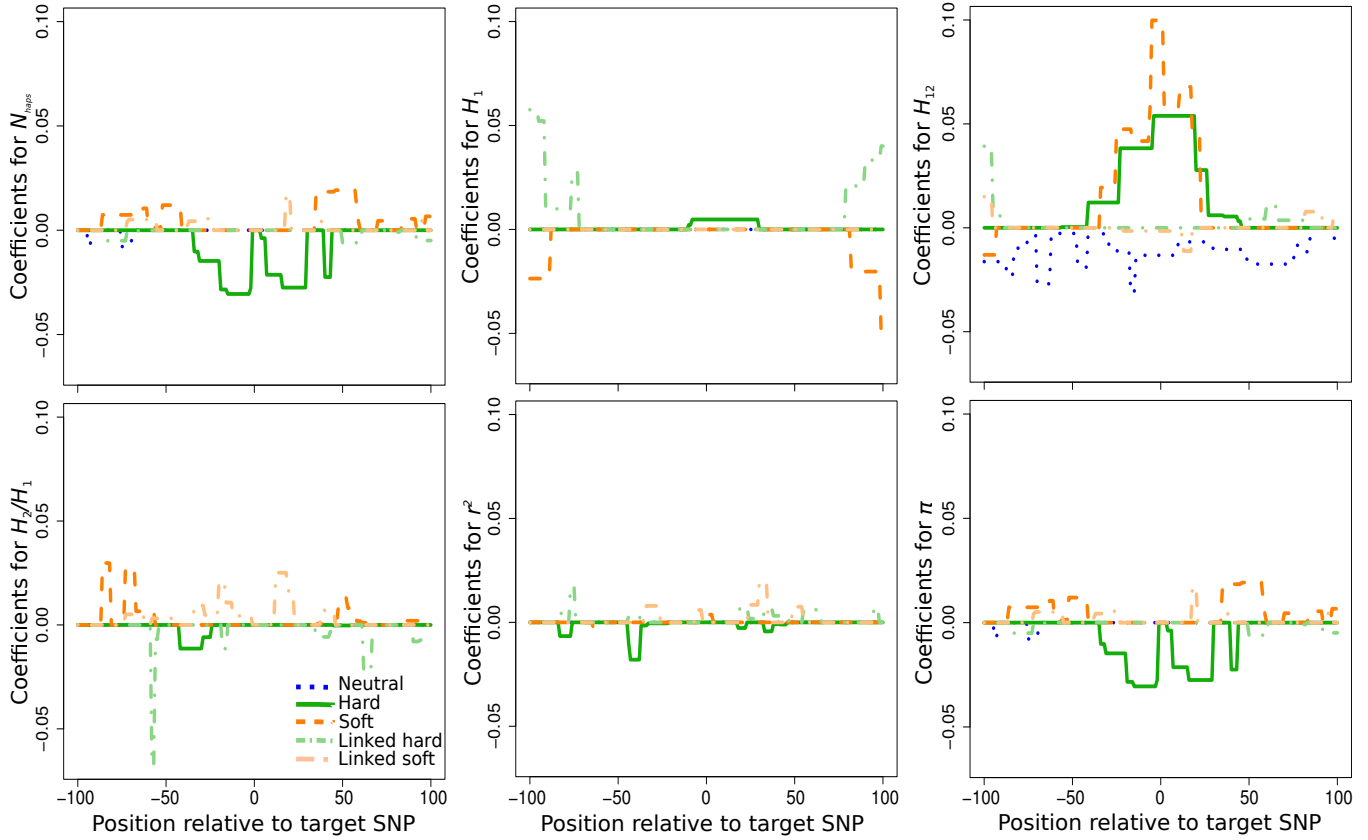


Figure S44: Spatial distributions of regression coefficients (β s) in neutral, hard sweep, soft sweep, linked to hard sweep, and linked to soft sweep scenarios for summary statistics N_{haps} , H_1 , H_{12} , H_2/H_1 , r^2 , and $\hat{\pi}$, for *Trendsetter* applied with a constant ($d = 1$) trend penalty. *Trendsetter* was trained on simulations with selection strength $s \in [0.005, 0.5]$ sampled uniformly at random on a log scale. Note that the distributions of regression coefficients for all summary statistics are plotted on the same scale, thereby making the distributions of some summaries difficult to decipher as their magnitudes are relatively small.

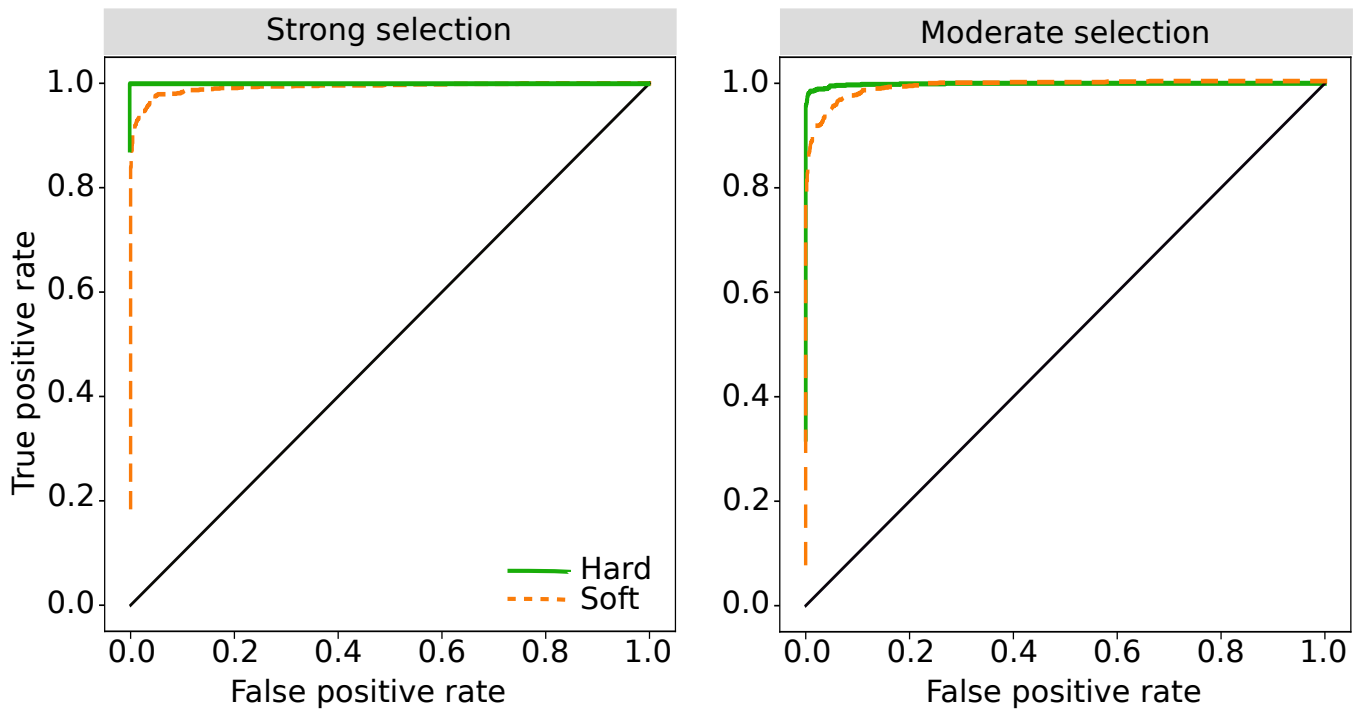


Figure S45: Receiver operating characteristic curves showing the power of *Trendsetter* with a constant ($d = 1$) trend penalty to detect hard and soft sweeps for strong ($s \in [0.05, 0.50]$) and moderate ($s \in [0.005, 0.050]$) selection, under a constant-size demographic history. For hard (soft) sweep curves, we compare the probability of a hard (soft) sweep under hard (soft) sweep simulations with the same probability under neutral simulations.